Energy Advances

ROYAL SOCIETY OF CHEMISTRY

REVIEW ARTICLE

View Article Online
View Journal | View Issue

Cite this: *Energy Adv.*, 2025, 4, 743

Composite revolution: unleashing the potential of polymers in sustainable energy and environmental applications

Arun Varghese, [ab] Kalathiparambil Rajendra Pai Sunajadevi *[ac] and Dephan Pinheiro [ac]

The rising demand for sustainable solutions to global energy and environmental challenges has accelerated research into advanced functional materials. Conductive polymer composites based on polyaniline (PANI), polypyrrole (PPy), poly(3,4-ethylenedioxythiophene) (PEDOT), and chitosan have emerged as promising candidates due to their tunable properties, environmental compatibility, and multifunctionality. This review highlights the energy and environmental applications of polymer-based mixed metal oxide catalysts. These composites show excellent performances in supercapacitance and water splitting applications, offering both efficient energy storage and hydrogen generation solutions and eco-friendly fuel alternatives. Using adsorption and corrosion inhibition techniques, water pollution and corrosion have also been addressed. Polymers such as PANI, PPy, PEDOT, and chitosan, when integrated with metal oxides, heteroatoms, and carbonaceous materials, enhance the functional properties of the composites. These materials demonstrate significant potential in supercapacitors, water splitting, adsorption, and corrosion resistance. The review provides a comparative analysis of different composites, helping readers understand how the incorporation of various components can improve performances. The review emphasizes sustainable approaches to tackle the current energy and environmental issues through advanced polymer-based catalytic systems.

Received 31st March 2025,
Accepted 20th April 2025

DOI: 10.1039/d5ya00088b

rsc.li/energy-advances

Introduction

The energy needs of the day are diverse and multifaceted, encompassing electricity generation, transportation, heating, cooling, and industrial processes.[1] Population growth, urbanization, and economic development continue to drive up energy demand globally, particularly in emerging economies. The march towards cleaner sources of energy, such as renewable energy and nuclear power, is essential to mitigate the environmental impact of fossil fuel consumption and combat climate change. Additionally, improving energy efficiency across sectors can reduce waste and enhance sustainability.[2–5]

Addressing society's energy and environmental needs requires navigating complex challenges and seizing opportunities for innovation and collaboration. Key challenges include decoupling the entrenched dependency on fossil fuels, improving the inadequate infrastructure for renewable energy deployment, overcoming the economic barriers towards sustainability initiatives, and bypassing geopolitical tensions over energy resources.[6,7]

The Sustainable Development Goals (SDGs), established by the United Nations in 2015, are a set of 17 interconnected targets aimed at addressing pressing global issues such as climate change, inequality, environmental degradation, and sustainable living (Fig. 1). SDG 6 focuses on clean water and sanitation, emphasizing universal access to safe water and

Fig. 1 Sustainable development goals declared by the United Nations. Reproduced from ref. 10 with permission from Wiley, copyright 2024.

[a] *Department of Chemistry, Christ University, Bangalore-560029, Karnataka, India. E-mail: sunajadevi.kr@christuniversity.in*
[b] *Department of Chemistry, Faculty of Engineering and Technology, Jain University, Bangalore 562112, India*
[c] *Centre for Renewable Energy and Environmental Sustainability, Christ University, Bangalore 560 029, India*

improved sanitation to prevent disease, improve quality of life, and support other SDGs.[8] With increasing water pollution and limited freshwater availability, technologies like adsorption and photocatalytic degradation are prioritized for effective water purification. Achieving SDG 6 not only improves health and ecosystems but also drives socio-economic growth, requiring collaborative action, innovative water technologies, and effective resource allocation.[9]

Similarly, SDG 7 promotes affordable and clean energy to ensure reliable and sustainable energy access.[11,12] This goal is crucial for powering essential services and transitioning from fossil fuels to renewable sources, despite challenges like poor infrastructure and funding. Technologies such as electrocatalytic water splitting for clean hydrogen production and supercapacitors for energy storage are pivotal to this shift.[13] Complementing these, SDG 9 emphasizes Industry, Innovation, and Infrastructure as pillars for economic and technological progress.[14] Advancements in supercapacitors, fuel cells, and water remediation methods support these goals by fostering innovation and sustainability. Ultimately, addressing energy and environmental challenges demands a holistic approach, combining technology, policy, and global cooperation to ensure a sustainable and resilient future.

As environmental concerns and global energy demands continue to rise, there is a greater emphasis on finding new materials that can meet these two issues. Polymer-based composites have become the most promising of the many materials being investigated because of their exceptional blend of adaptability, adjustable characteristics, and functional performance. Particularly, bio-derived polymers like chitosan and conductive polymers like polyaniline (PANI), polypyrrole (PPy), and poly(3,4-ethylenedioxythiophene) (PEDOT) have attracted a lot of interest. When combined or utilized separately, these materials present encouraging opportunities for the creation of multipurpose platforms designed for environmentally friendly energy conversion and clean-up.[15,16]

S. Peter *et al.* reported a review on the usage of chitin and chitosan in energy and environmental applications.[17] A review of the energy storage applications of biopolymers like cellulose, chitosan, and lignin is also reported.[18] A comparative study of the usage of polymers supported nanocomposites in environmental applications was reported by X. Zhao and coworkers.[19] A review of the nanocellulose based polymers is reported for energy conversion applications.[20] A study on carbon based polymer nanocomposites was reported for energy storage applications.[21] A review of functionalized nanoparticle loaded polymers for water splitting, solar cells, and carbon dioxide capture studies was also reported.[22] A comparison table of various reported reviews is given in Table 1. In this review, we have focused on the various polymer composites like PANI, PPy, PEDOT, and chitosan composites for applications like supercapacitance, electrocatalytic water splitting, adsorption, and corrosion inhibition studies. A comprehensive study of these different polymers for four different applications in a single review will be of great help to researchers who are in their early stages. The discussions on sustainable development goals are also included in the review. Detailed descriptions of the applications and the importance of polymer based composites are carried out in the study. Finally, comparative studies on the usage of these composites for various energy and environmental applications are given in the review. As we strive for sustainable development, we must explore innovative technologies that meet our energy needs and minimize the environmental impact. This is where the pivotal role of supercapacitors, water splitting, corrosion, and adsorption studies in addressing these critical issues acquires significance.

Energy and environmental applications

Supercapacitors

Supercapacitors, also known as ''ultracapacitors'' or ''electrochemical capacitors,'' have emerged as effective storage devices of energy due to their high power and energy density, rapid charging capabilities, and excellent stability. Unlike conventional capacitors that store energy through electrostatic attraction between opposite charges on conductive plates, supercapacitors utilize electrochemical double-layer capacitance (EDLC) or pseudocapacitance mechanisms. These mechanisms empower supercapacitors to achieve significantly higher energy densities compared to conventional capacitors while offering rapid charge and discharge rates akin to batteries.[23,24] At the core of supercapacitor technology lies the development of an electrochemical double layer at the interface between an electrode and an electrolyte solution. When a voltage is applied across the electrodes immersed in the electrolyte, ions from the electrolyte crowd around the electrode–electrolyte interface and create a double layer of charges. This process occurs swiftly and is reversible, enabling supercapacitors to exhibit high power density characteristics crucial for applications requiring rapid energy storage and release cycles.[25]

Supercapacitors store electrical energy through two primary mechanisms: electrostatic double-layer capacitance and pseudocapacitance. Electrostatic double-layer capacitance involves

Table 1 Comparison of reported reviews with the present study

Sl. no.	Composite	Applications	Ref.
1	Chitin and chitosan	Energy and environmental	17
2	Biopolymers	Energy storage	18
3	Polymers supported nanocomposites	Catalytic degradation and sensing	19
4	Nanocellulose based composites	Energy conversion devices	20
5	Carbon based polymers	Energy storage studies	21
6	Functionalized nanoparticle loaded polymers	Water splitting, solar cells, CO_2 capture	22
7	Polyaniline, polyoyrrole, PEDOT, and chitosan	Supercapacitance, water splitting, adsorption, and Corrosion inhibition	This study

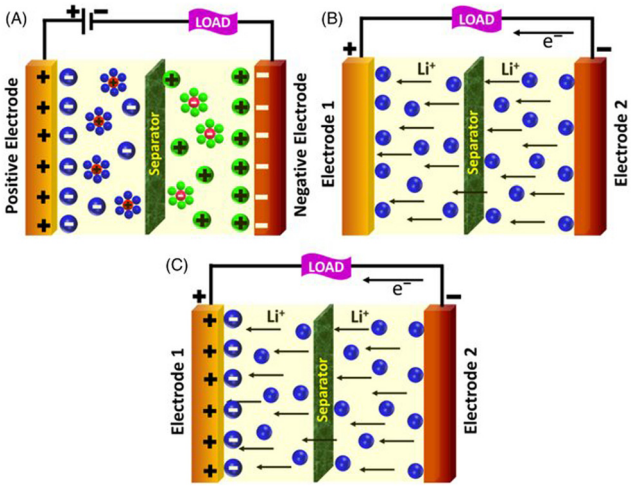

Fig. 2 (A) EDLC (B) pseudo and (C) hybrid supercapacitors. Reproduced from ref. 28 with permission from Wiley, copyright 2022.

the physical separation of charges at the electrode–electrolyte interface. Similar to static electricity storage in conventional capacitors, this mechanism is significantly enhanced by utilizing high-surface-area electrode materials and efficient electrolytes.[26] Meanwhile, pseudocapacitance involves redox reactions at the electrode surface, where ions in the electrolyte undergo faradaic processes, leading to additional charge storage. This mechanism, which is akin to batteries but distinguished by faster charge transfer kinetics, complements electrostatic double-layer capacitance to achieve higher energy densities. Common pseudocapacitive materials in supercapacitors include transition metal oxides and conducting polymers, known for their higher capacitance values than purely electrostatic storage.[27] The combination of these mechanisms gives rise to another type of supercapacitor called hybrid supercapacitor.[28] The types of supercapacitors are illustrated in Fig. 2. The choice of electrode materials heavily influences the performance characteristics of supercapacitors. Carbon-based materials such as graphene compounds, activated carbon, and carbon nanotubes dominate due to their high specific surface area, excellent electrical conductivity, and chemical stability in various electrolytes. These materials facilitate the efficient formation of the electrostatic double-layer and contribute significantly to the high capacitance values and rapid charge–discharge capabilities of supercapacitors.[29]

Supercapacitors find diverse applications across industries and technological domains owing to their unique attributes. In renewable energy systems, supercapacitors serve as energy storage devices for mitigating power output fluctuations from solar panels and wind turbines. Supercapacitors also enhance portable electronic devices, acting as auxiliary power sources during peak demand periods, thereby extending battery life and improving device performance.[30,31] In transportation, supercapacitors enhance the efficiency of regenerative braking systems in electric vehicles by swiftly storing and releasing energy during braking cycles. This not only enhances vehicle efficiency but also prolongs battery life by reducing stress on the energy storage system.[32] Additionally, supercapacitors are integral to hybrid electric vehicles, providing bursts of high power for acceleration and complementing the energy density of batteries. The integration of supercapacitors into electronics and consumer goods optimizes energy management systems and enable innovative functionalities like rapid charging for mobile devices, instantaneous energy storage for wearable electronics, and reliable backup power for critical equipment. Their ability to operate across a wide temperature range and endure numerous charge–discharge cycles makes supercapacitors suitable for demanding environments where durability and reliability are paramount.[33]

Supercapacitor applications span transportation, renewable energy, electronics, and industrial sectors, contributing to enhanced energy efficiency, reduced environmental impact, and the emergence of new technological innovations.[34,35] Advancements in supercapacitor technology continue to be driven by research aimed at improving energy density, enhancing power density, and optimizing cost-effectiveness. Innovations in electrode materials, electrolyte formulations, and device architecture pave the way for supercapacitors with higher energy storage capacities and extended operational lifetimes. Emerging trends include the development of flexible supercapacitors for wearable electronics, the integration of supercapacitors into structural components for smart materials applications, and the exploration of hybrid systems that combine the strengths of supercapacitors and batteries. As research continues to push the boundaries of supercapacitor performance and scalability, these devices are poised to play a pivotal role in transforming our society towards a sustainable energy future.

Electrocatalytic water splitting

Electrocatalytic water splitting, or electrolysis, is a process that uses electrical energy to decompose water into hydrogen and oxygen gases. Hydrogen, known as the cleanest form of energy, holds tremendous potential as a versatile fuel source for transportation, power generation, and industrial applications.[36,37] However, the widespread adoption of hydrogen fuel faces cost, efficiency, and infrastructure challenges. Through rigorous research and development in water splitting studies, scientists aim to overcome these barriers by improving catalysts, electrolytes, and system design. By leveraging advances in water splitting technology, we can harness the abundant energy of sunlight or renewable electricity to produce clean hydrogen fuel, thereby reducing our dependence on fossil fuels. Electrocatalytic water splitting stands at the forefront of renewable energy conversion, aiming to harness electricity from sustainable sources to produce clean hydrogen fuel. This process involves intricate mechanisms encompassing both the hydrogen (HER) and oxygen evolution reactions (OER).[38,39] The electrocatalytic overall water splitting studies produce hydrogen and oxygen gases by lowering the activation energy barriers for HER and OER using the electrocatalysts.[40]

The HER starts with the reduction of protons (H^+) from water to form hydrogen gas (H_2). There are three steps in the mechanism of HER leading to the production of hydrogen in a basic medium. Volmer step (eqn (1)), Heyrovsky step (eqn (2)), and Tafel step (eqn (3)) are the three basic steps in hydrogen

production. The Tafel slope values for the Volmer, Heyrovsky step, and Tafel reaction steps are 120, 40, and 30 mV dec^{-1}, respectively.[41]

$$H_3O^+ + e \rightarrow H_{ads} + H_2O \quad (1)$$

$$H_3O^+ + H_{ads} + e \rightarrow H_2 + H_2O \quad (2)$$

$$H_{ads} + H_{ads} \rightarrow H_2 \quad (3)$$

This reaction predominantly takes place on the catalyst surface, where protons from the aqueous electrolyte solution adsorb onto active sites. The process involves the adsorption of protons, followed by the transfer of electrons present in the external circuit to the catalyst surface, facilitating the reduction of protons to hydrogen atoms. These hydrogen atoms subsequently combine to form H_2 molecules, which desorb from the catalyst surface into the gas phase. The effectiveness of the HER is contingent upon several factors, including the catalyst's active sites, surface area, electronic structure, and interactions with the electrolyte. Catalysts with optimized properties enhance the kinetics of hydrogen production.

In water electrolysis, OER occurs at the anode with a thermodynamic voltage of 1.23 V, while the HER happens at the cathode with a thermodynamic voltage of 0 V. The total voltage required for water decomposition in electrolysis is 1.23 V.[42,43] The schematic representation of overall water splitting is given in Fig. 3.

In an alkaline medium, the HER taking place at the cathodic site is given by eqn (4).

$$2H^+ + 2e \rightarrow H_2 \quad (4)$$

The OER taking place at the anode is given by eqn (5).

$$H_2O \rightarrow 2H^+ + \frac{1}{2}O_2 + 2e \quad (5)$$

The overall water splitting reaction is given by eqn (6).

$$2H_2O \rightarrow 2H_2 + O_2 \quad (6)$$

The optimization of electrocatalytic overall water splitting involves balancing the performance of HER and OER catalysts to maximize hydrogen production efficiency. Strategies for improving efficiency include innovative design and engineering of the catalyst to enhance active sites and surface areas for both reactions. Additionally, electrolyte optimization plays a critical role in facilitating proton and ion transport while mitigating parasitic reactions and catalyst degradation. Fine-tuning operational conditions such as pH, temperature, and applied potential further enhances catalyst activity and stability over extended electrochemical cycles.

Research in electrocatalytic overall water splitting continues to advance through the development of novel materials, deeper insights into reaction mechanisms, and the scaling up of electrochemical systems for practical applications. By leveraging the synergistic effects of materials science, electrochemistry, and renewable energy technologies, electrocatalytic overall water splitting represents a cornerstone in enabling a sustainable hydrogen economy and addressing global energy challenges.[44,45] The electrocatalytic HER holds significant importance within electrochemistry, particularly in advancing technologies aimed at generating clean hydrogen fuel from water using renewable energy sources. This reaction is pivotal across various applications such as water electrolysis, hydrogen fuel cells, and renewable energy storage, where efficient and sustainable hydrogen production is crucial.

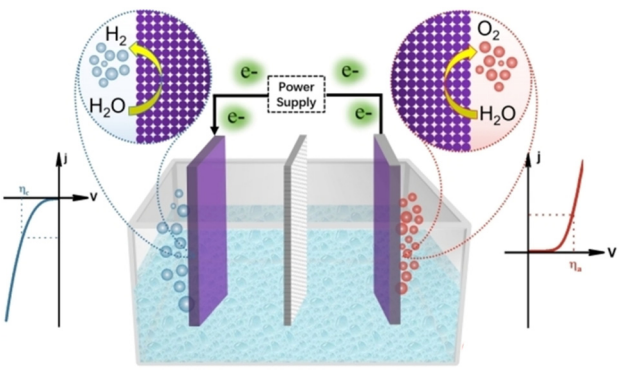

Fig. 3 Schematic representation of overall water splitting. Reproduced from ref. 43 with permission from Wiley, copyright 2021.

Adsorption studies

Adsorption is a process where molecules or ions from a fluid phase adhere to the surface of a solid or liquid, known as the adsorbent. This phenomenon arises from the attractive forces between the adsorbate and the surface of the adsorbent.[46] Various factors, including the nature of the adsorbate and adsorbent, surface properties, temperature, pressure, and the presence of other substances in the fluid phase, influence the adsorption mechanisms. Adsorbent materials, such as conducting polymers, activated carbon, zeolites, and metal–organic frameworks, exhibit high surface areas and optimized pore structures, enabling efficient removal of pollutants, contaminants, and toxins from air and water.[47,48] Adsorption studies focus on optimizing adsorbent materials, understanding adsorption mechanisms, and designing cost-effective treatment processes. By leveraging the power of adsorption, we can address pressing environmental challenges, such as air pollution, water scarcity, and contamination, while promoting public health and ecological sustainability.[49–52] A graphical representation of the adsorption process is shown in Fig. 4.

Understanding adsorption mechanisms is pivotal to numerous scientific disciplines, encompassing chemistry, materials science, environmental science, and engineering. It serves as the foundation for applications spanning purification and separation processes, catalysis, drug delivery systems, and ecological remediation strategies.[53,54] Adsorption can be broadly categorized into physical and chemical adsorption, each characterized by distinct mechanisms and energetics.[55] External factors such as temperature and pressure also impact adsorption mechanisms. In physical adsorption, lower temperatures typically favour adsorption because they decrease the thermal energy available to adsorbate molecules, enhancing their likelihood to adhere to the adsorbent surface.

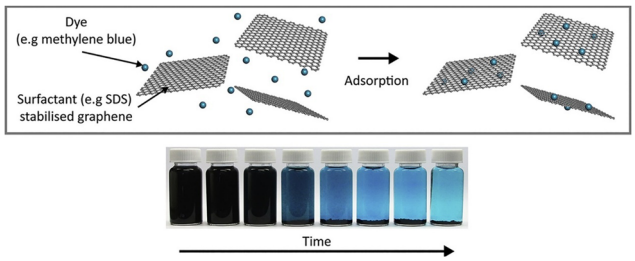

Fig. 4 Schematic representation of adsorption of dye molecules using graphene. Reproduced from ref. 53 with permission from Elsevier, copyright 2018.

Conversely, in chemisorption, higher temperatures may facilitate the activation of chemical bonds, thereby promoting adsorption. Pressure influences adsorption by altering the concentration of adsorbate molecules in the fluid phase and affecting adsorbate–adsorbent interactions.[56] Physical adsorption, or physisorption, entails relatively weak intermolecular forces like van der Waals forces, hydrogen bonding, and dipole–dipole interactions between the adsorbate molecules and the surface of the adsorbent. These forces arise due to temporary or induced dipoles in both the adsorbate and adsorbent materials. Physisorption is typically non-specific and reversible, occurring on any surface irrespective of its chemical composition. The strength of physisorption increases with rising surface area and diminishes with temperature, as higher temperatures provide adequate thermal energy to overcome weak van der Waals forces, thereby causing desorption of the adsorbate molecules.[57] Chemical adsorption, or chemisorption, on the other hand, involves stronger interactions between the adsorbate and the surface of the adsorbent, often through chemical bonds such as ionic, covalent, or metallic bonds. Chemisorption necessitates a specific chemical affinity between the adsorbate and the surface, frequently involving electron transfer or sharing between molecules and surface atoms or ions. This type of adsorption is typically more specific and irreversible compared to physisorption. Chemisorption processes often demand activation energy to initiate bond formation or breaking, which can be influenced by factors such as temperature, pressure, and the presence of catalysts.[46,58]

The adsorbent surface's physical and chemical properties, surface area, porosity, surface charge, and surface functional groups are critical in determining adsorption capacity and selectivity. Higher porosity and surface area provide more efficient active sites for adsorption, whereas surface charge and functional groups can influence interaction strength and specificity between the adsorbent and adsorbate molecules.[59] The study of adsorption mechanisms often employs advanced experimental techniques and theoretical models to elucidate the underlying processes. Experimental methods encompass isotherm studies, measuring equilibrium adsorption capacity as a function of adsorbate concentration at constant temperature, and kinetic studies, examining the rate at which adsorption equilibrium is achieved over time. Adsorption mechanisms are multifaceted and dependent on a complex interplay of factors, including intermolecular forces, surface properties, temperature, pressure, and chemical affinity.[60] Understanding these mechanisms is essential for designing and optimizing adsorption processes across various industries, such as environmental remediation, water purification, gas separation, catalysis, and biomedical applications. Advancements in experimental techniques and theoretical modelling continuously expand the knowledge of adsorption mechanisms, paving the way for innovative solutions to global challenges in sustainability and public health.[61]

Corrosion inhibition studies

Corrosion, the gradual degradation of materials due to chemical reactions with the environment, poses significant challenges to infrastructure integrity, safety, and environmental sustainability. From pipelines and bridges to industrial equipment and marine structures, corrosion costs billions of dollars annually and poses risks to public health and the environment. Corrosion studies play a vital role in understanding the mechanism of corrosion and developing effective mitigation strategies, such as protective coatings, corrosion inhibitors, and advanced materials. By combating corrosion, we can prolong the lifespan of infrastructure, conserve resources, and minimize environmental pollution, contributing to savings in cost, sustainable development, and economic prosperity.[62]

Electrochemical corrosion inhibition studies encompass a wide range of research focused on mitigating the damaging effects of corrosion on metallic materials. Corrosion, an electrochemical process, results in the deterioration of metals through oxidation reactions in the presence of an electrolyte. This issue presents significant challenges across various sectors, such as transportation, infrastructure, marine, and aerospace industries, where metal structures are constantly exposed to harsh environmental conditions. The primary goal of corrosion inhibition studies is to devise effective strategies and materials that can reduce corrosion rates and prolong the lifespan of metal components.[63] The foundation of electrochemical corrosion inhibition studies lies in comprehending the underlying mechanisms and dynamics of corrosion process. Corrosion typically proceeds through simultaneous anodic dissolution and cathodic reactions on metal surfaces immersed in electrolytes. Anodic dissolution involves the release of metal ions into the electrolyte solution, while cathodic reactions, such as oxygen reduction or hydrogen evolution, consume electrons to maintain charge equilibrium. This electrochemical nature of corrosion forms the basis for evaluating the efficacy of corrosion inhibitors.[64,65] A schematic representation of corrosion inhibitor on copper substrate is shown in Fig. 5.

One of the fundamental techniques employed in electrochemical corrosion inhibition studies is electrochemical impedance spectroscopy (EIS). EIS enables the characterization of the electrical properties of metal–electrolyte interfaces by measuring impedance responses across a range of frequencies. Analyzing impedance spectra helps researchers understand how inhibitors modify the electrochemical behavior of metal surfaces, thereby impeding corrosion processes. Another widely used method in corrosion inhibition studies is potentiodynamic polarization.

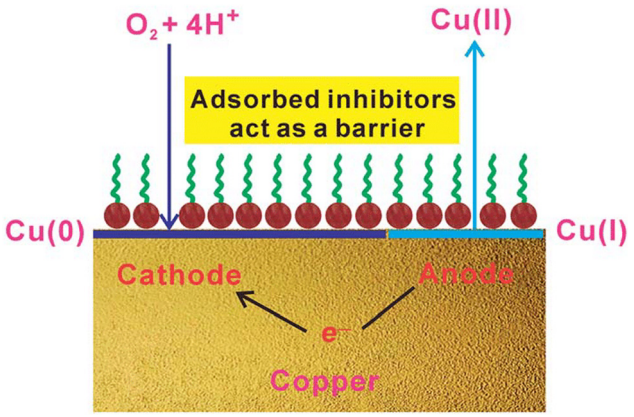

Fig. 5 Schematic representation of corrosion inhibition on copper surface. Reproduced from ref. 65 with permission from RSC, copyright 2014.

By comparing polarization curves obtained with and without inhibitors, researchers can quantify the extent to which inhibitors suppress corrosion rates and shift the corrosion potential towards more noble values. This information is critical for elucidating the mechanism of action of inhibitors and optimizing their formulation for practical applications.[66,67]

The selection and design of corrosion inhibitors play a pivotal role in electrochemical corrosion inhibition studies. Corrosion inhibitors are chemical compounds or coatings that adsorb onto metal surfaces, forming protective barriers that impede the electrochemical reactions responsible for corrosion. The effectiveness of inhibitors hinges on several factors, including their chemical composition, molecular structure, adsorption affinity to metal surfaces, and ability to modify corrosion potential and current density (C_D).[68] Organic compounds such as organic acids, amines, polymers, and heterocyclic compounds are commonly employed as corrosion inhibitors due to their capacity to form stable complexes with metal ions or adsorb onto metal surfaces through non-covalent interactions. Inorganic inhibitors, such as metal oxides, chromates, phosphates, and molybdates, are also utilized for their ability to develop passive oxide layers on metal surfaces, thereby preventing further corrosion.[69,70] Hybrid inhibitors, which integrate organic and inorganic components, have gained attention for their synergistic effects in enhancing corrosion protection. Designing effective inhibitors involves a systematic approach encompassing screening candidate compounds through laboratory tests, evaluating their performance under simulated environmental conditions, and optimizing their formulation for specific applications.[71] The evaluation of corrosion inhibitors extends beyond laboratory experiments to encompass field studies and practical applications. Accelerated corrosion testing methodologies, including salt spray testing, humidity chamber testing, and immersion testing in corrosive environments, are utilized to simulate severe operating conditions and assess the durability of inhibitors over extended periods.[72]

The significance of electrochemical corrosion inhibition studies transcends corrosion control to encompass broader implications for sustainability, safety, and economic viability. By reducing corrosion rates and extending the service life of metal structures, corrosion inhibitors contribute to substantial cost savings associated with the maintenance, repair, and replacement of corroded components. Moreover, corrosion inhibition is crucial in bolstering the reliability and safety of critical infrastructure such as bridges, pipelines, offshore platforms, and industrial equipment, thereby minimizing the risk of catastrophic failures and environmental contamination.[73] Electrochemical corrosion inhibition studies epitomize a multidisciplinary field that integrates chemistry, materials science, electrochemistry, and engineering principles to devise effective strategies for mitigating corrosion in diverse industrial applications. Through advanced electrochemical techniques and systematic evaluation methodologies, researchers continue to innovate and optimize corrosion inhibitors to meet the evolving demands of modern industries for sustainable and resilient infrastructure. As the global emphasis on environmental sustainability and resource conservation grows, the development of effective corrosion inhibitors and their applications is set to play a pivotal role in ensuring the longevity and performance of metallic materials across a wide spectrum of challenging environments.

Polymer based composites for energy and environmental applications

Conducting polymers are polymers with highly π-conjugated polymeric chains and are also called 'synthetic metals.' Some of the important conducting polymers used are polyacetylene, polyaniline (PANI), polypyrrole (PPy), polythiophene, poly(*para*-phenylene), chitosan, poly(3,4-ethylenedioxythiophene) (PEDOT), and polyfuran. These conducting polymers have readily tunable bandgaps, good redox chemistry or electroactivity, high flexibility, and good processability over inorganic nanomaterials.[74] The studies on conducting polymers started in the 1970s.[75] The polymer-based nanocomposites are prepared by reinforcing polymers with nanoparticles. Nanoparticles have strong activation and inter-particle interactions, which lead to strong aggregation tendencies that hinder the possibilities of exploring the properties and applications. This can be avoided by coating or grafting polymers onto the nanoparticle surface; thus, the polymers can hold the functional groups of nanoparticles, which prevents their aggregation.[76]

PANI, a conducting polymer, when combined with TiO_2 nanocomposite, shows enhanced energy applications like photocatalysis, energy storage, anti-corrosion, and supercapacitance.[77,78] Polyvinyl alcohol and chitosan have gained the attention of scientists due to their less expensive, non-toxic, biodegradable, non-carcinogenic, bio-compatible, and water-soluble properties.[79,80] PVA was combined with TiO_2 to produce good photocatalytic and antibacterial results.[81] Polymeric carbon nitride is a semiconductor that has a bandgap of 5 eV.[82] It is the oldest synthetic polymer reported, showing high photocatalytic activity for hydrogen production and good absorption properties in the range of visible light. These carbon nitride-sensitized TiO_2 nanotube arrays showed significantly improved photoelectrochemical and photocatalytic properties than

TiO_2 nanotube arrays.[83] Z–Z-scheme heterojunction photocatalyst was made by the combination of polypyrrole, Ag, and inorganic particles. Conductive polymer, PPy, has high absorption coefficients in visible light, increased mobility of charges, and good environmental stability. This was doped with silver (Ag) since it can act as an electron mediator.[84] Polyaniline was combined with zinc oxide and copper oxide to degrade organic pollutants. In another study, polyaniline was combined with TiO_2 and CuO for degradation of 4-chlorophenol.[85,86]

Antibacterial studies of polymer-based nanocomposites have been conducted.[87] Polyvinyl alcohol was combined with magnesium oxide and silicon carbide, which showed better antibacterial properties.[88] Polypyrrole chitosan composite showed high inhibition rates against *E. coli* bacteria.[89] PANI is another important polymer used in antibacterial studies of polymer-based nanocomposites.[90]

Conducting polymers-based supercapacitors are made from PANI, polypyrrole, and polythiophene.[91] Supercapacitors created by combining PANI with graphene showed higher capacitance than individual PANI and graphene.[92] PANI is lightweight, low cost, high conductivity, has good flexibility, and is environmentally friendly. Combining PANI with metal oxides will enhance their cyclic stability. Polypyrrole is another conducting polymer with safety excellent conductivity and higher density than other CPs.[93] Heavy metals, like cobalt, cadmium, chromium, and lead, have been absorbed from aqueous solutions using polymers and polymer composites. Polymers like PANI and PPy combine with other metal oxides, like SiO_2 and TiO_2, to perform adsorption activities.[94,95] Polyvinyl alcohol-based composites have been used to study adsorption properties to remove copper ions from an aqueous solution.[96] Polymer-based nanocomposites were also used for corrosion studies.[62] Polyvinyl acetate and PANI were effectively used in corrosion resistance studies.[97]

Recently, various studies on polymer-based mixed metal oxides have been reported. Polypyrrole–CuO–ZnO composites were used for oxygen-sensing studies.[98] PANI–CuO–TiO_2–SiO_2 composites were used for ammonia sensing studies.[99] PANI–CuO–ZnO composites were used in degradation studies.[86] PANI–CuO–TiO_2 composites were used for the degradation of 4-chlorophenol. In another study, PANI–ZnO–CuO composites were used for the degradation of organic pollutants.[85,86]

The combination of conducting polymers with suitable elements will enhance functionality due to the synergy between the elements, and efficient composites can be fabricated for various energy and environmental applications. Polymer based composites are used in various energy and environmental applications. Polymers like PANI,[100] PPy,[101] PEDOT,[102] and chitosan[103] have been explored widely by scientists for different applications. The excellent surface area, conductive nature, and redox properties make them better candidates for energy and environmental applications. Incorporating these polymers with various substances like metal, metal oxides, and heteroatoms gives rise to efficient composites and is used in supercapacitance, electrocatalytic water splitting, adsorption, and corrosion inhibition studies. The energy and environmental needs of society require multifaceted solutions that integrate scientific innovation, technological advancement, and ecological safety. Supercapacitors, water splitting, corrosion, and adsorption studies are critical for addressing these complex challenges and for shaping a more sustainable future. Investing in research, education, and collaboration can harness these technologies' transformative potential to meet society's evolving needs while safeguarding the planet for future generations.

Polyaniline composites for energy and environmental applications

In 1834, Ferdinand Runge reported the polymerization of aniline to get aniline black. However, PANI did not attract significant scientific attention until the 1980s, spurred by pioneering research on conductive polymers by Alan J. Heeger, Alan G. MacDiarmid, and Hideki Shirakawa, which eventually earned them the Nobel Prize in Chemistry in the year 2000.[104] PANI's conductive properties are highly dependent on its oxidation state, which can be adjusted through doping processes. This versatility makes PANI particularly appealing for various applications. Among the earliest and most impactful uses of PANI is in energy storage, notably in rechargeable batteries and supercapacitors. PANI's high conductivity and environmental stability enhance the performance and longevity of these devices. Additionally, its ability to undergo reversible redox reactions makes it an excellent candidate for electrode materials in batteries and supercapacitors.[105]

In environmental applications, PANI has shown considerable promise in removing pollutants from water and air. It can adsorb and degrade organic pollutants, heavy metals, and dyes, making it an effective material for environmental remediation. Furthermore, PANI's conductive nature allows it to be used in sensors for detecting environmental toxins and pollutants, enabling real-time monitoring of environmental quality.[106] The combination of PANI with other compounds, such as graphene and metal oxides, has led to the creation of advanced composites with enhanced properties for both energy and environmental applications. These composites often demonstrate improved electrical conductivity, mechanical strength, and chemical stability.[107] The evolution of PANI from a chemical curiosity to a pivotal material underscores the importance of interdisciplinary research and innovation. As researchers continue to discover new ways to improve the properties and performance of PANI, its role in addressing some of the most critical energy and environmental challenges of our time is likely to expand further.

Polyaniline composites for supercapacitance studies

Various metal oxides were combined with PANI to be used as electrodes for supercapacitor applications. Iron oxide derived from the used ink cartridges was combined with PANI, which showed a specific capacitance (C_{SP}) of 286 F g^{-1} when 4 M KOH was used as the electrolyte.[100] The electrochemical polymerization method was used to fabricate the PANI/molybdenum oxide working electrode on carbon cloth. This material showed a C_{SP} of 841.6 F g^{-1} at a C_D of 0.5 A g^{-1}.[108] A C_{SP} of 376 F g^{-1} and a capacitance retention of 95.3% after 10 000 cycles were realised for a working electrode made of PANI and copper oxide.[109]

D. J. Ahirrao *et al.* have studied the efficiency of PANI/manganese oxide composite, which showed a C_{SP} of 605 F g^{-1} at a C_D of 1 A g^{-1}. In this study, the PANI showed a C_{SP} of 515 F g^{-1}, and manganese oxide showed a C_{SP} of 141 F g^{-1}.[110] D. A. L. Almeida *et al.* studied the effect of PANI's energy storage efficiency by incorporating various metal oxides like iron, nickel, and manganese. Out of these, they found that PANI/manganese oxide composites showed a comparatively higher efficiency with a C_{SP} of 115.7 F g^{-1}.[111] PANI/CuO composite utilized for energy storage studies showed a C_{SP} of 424 F g^{-1} (Fig. 6).[112]

In another study, zinc cobalt oxide was combined with PANI to give a C_{SP} of 1055 F g^{-1} at 1 A g^{-1} and capacitance retention of 85.7% at 10 000 cycles.[113] PANI was combined with cobalt oxide to give a C_{SP} of 985 F g^{-1}, whereas pristine cobalt oxide showed a C_{SP} of 278 F g^{-1}.[114] When PANI was combined with manganese oxide, the C_{SP} value demonstrated was 323.7 F g^{-1} at a scan rate of 5 mV s^{-1}.[115] In another study, PANI combined with iron oxide showed a C_{SP} of 572 F g^{-1} at a C_D of 0.5 A g^{-1}.[116] M. M. Mezgebe *et al.* evaluated the efficiency of PANI with manganese oxide and found it to have a C_{SP} of 665 F g^{-1} (Fig. 7a–d).[117] PANI combined with cobalt oxide has shown a C_{SP} of 1151 F g^{-1} at a C_D of 3 A g^{-1}, with a capacitance retention of 92% at 5000 cycles.[118]

Different compounds like metal–organic framework (MOF), graphene oxide (GO), and reduced graphene oxide (rGO) were combined with PANI and metal oxides to form ternary composites. These composites were used as electrodes for energy storage studies. D. Qin *et al.* have studied the energy storage capacity of PANI combined with ZnO and Zn–Co MOF and observed a C_{SP} of 458.9 F g^{-1} at a C_D of 1 A g^{-1}. They have also constructed an asymmetric supercapacitor with activated carbon as the anionic electrode and the studied material as the cationic electrode.[119] When PANI was combined with copper oxide and rGO, a C_{SP} of 534.5 F g^{-1} was shown at a C_D of 1 A g^{-1}.[120] PANI, when combined with titanium oxide and tin oxide, showed a C_{SP} of 540 F g^{-1}. This composite showed a

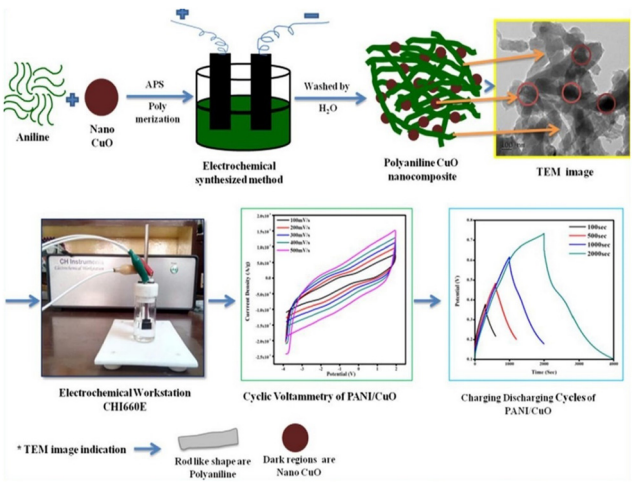

Fig. 6 The supercapacitance analysis using PANI/CuO composite. Reproduced from ref. 112 with permission from Elsevier, copyright 2020.

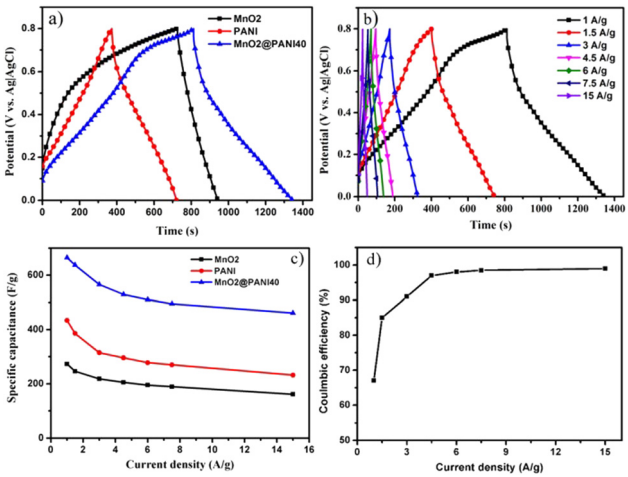

Fig. 7 The galvanostatic charge–discharge graphs of PANI/manganese oxide composite evaluated for charge storage capacity. Reproduced from ref. 117 with permission from Elsevier, copyright 2019.

capacitance retention of 85% after 6000 cycles.[121] K. Y. Yasoda *et al.* combined PANI and manganese oxide with GO, which showed a C_{SP} of 829 F g^{-1}. The presence of GO has increased the efficiency of PANI towards energy storage.[122] PANI incorporated with nickel ferrite spinel in 1 : 1 weight ratio has shown a maximum C_{SP} of 758 F g^{-1}. It showed a maximum capacitance retention of 97% at 10 000 cycles.[123] A composite having a core–shell intercalation structure was synthesized by Y. Ma *et al.* The composite was PANI/manganese oxide/nickel oxide with GO. A C_{SP} of 396 F g^{-1} at a C_D of 0.5 A g^{-1}. It also showed a cyclic stability of 82.6% at 3000 cycles.[124] PANI, when combined with nickel cobalt oxide, showed a C_{SP} of 561.2 F g^{-1} at 10 A g^{-1}. This was combined with a negative MXene electrode for an asymmetric supercapacitor, which showed a cyclic stability of 86.2% at 3000 cycles. The efficient redox kinetics and better dynamic equilibrium between the positive and negative electrodes in the two-electrode system are responsible for the energy storage capacity.[125] PANI combined with manganese oxide and N-doped carbon showed a specific capacity (C_S) of 410 C g^{-1}. When manganese oxide was replaced with tin oxide, the C_S value increased to 534 C g^{-1}. Both the composites showed more than 97% capacitance retention after 5000 cycles.[126] PANI/GO combined manganese and molybdenum oxide was used as a working electrode for electrochemical analysis of energy storage. The C_{SP} of this electrode was found to be 596 F g^{-1}.[127]

A hierarchical porous ruthenium cobalt oxide combined with PANI composite was utilized as the working electrode to study the efficiency of energy storage. This composite demonstrated a C_S of 1028.7 C g^{-1} at a C_D of 1 A g^{-1}. This composite also showed a high capacity retention of 93.2% even after 10 000 cycles.[128] The prepared PANI/copper manganite composite working electrode by A. S. A. Almalki showed a C_{SP} of 1181 F g^{-1} at a C_D of 1 A g^{-1} and demonstrated 95% capacitance retention at 5000 cycles.[129] PANI/nanowire-shaped cobalt oxide grown on nickel foam was used as an electrode for an asymmetric supercapacitor, which showed a C_S of 1113 C g^{-1} at a C_D of 3 A g^{-1}.

The cyclic stability showed by this composite was 86.3% at 10 000 cycles.[130] In another study, PANI/cobalt oxide combined with rGO showed an enhanced capacitance of 1982 F g^{-1} when a scan rate of 10 mV s^{-1} was employed. The device fabricated using a two-electrode system shows a C_{SP} of 662 F g^{-1} at a C_D of 1 A g^{-1}.[131] PANI was combined with oxides of nickel, cobalt, and praseodymium to study the efficiency of energy storage. It was seen that the synthesized composite gave a C_{SP} of 905 F g^{-1} at a C_D of 1 A g^{-1}.[132] PANI combined with molybdenum oxide showed a C_{SP} of 606 F g^{-1} at a C_D of 1 A g^{-1}.[133] Ni–Co–Mn MOF combined with rGO and PANI has shown a C_{SP} of 1007 F g^{-1} at a C_D of 1 A g^{-1}.[134]

PANI combined with various metal oxides has shown substantial promise as an electrode material for supercapacitor applications, owing to its high pseudocapacitance and environmental stability. Notably, composites such as PANI/zinc–cobalt oxide (1055.0 F g^{-1}), PANI/ruthenium–cobalt oxide (1028.7 F g^{-1}), and PANI/Ni–Co–Mn–MOF/rGO (1007.0 F g^{-1}) demonstrated superior C_{SP} values due to the synergistic effects between the redox-active metal oxides and the conductive polymer matrix. The integration of binary and ternary metal oxides, as well as the inclusion of conductive additives like rGO, enhances the charge storage capability, cycling stability, and surface area of the composites. Overall, PANI-based hybrid materials emerge as efficient candidates for high-performance supercapacitors, especially when tailored with multi-component oxide systems.

Polyaniline composites for water splitting studies

Composites containing PANI have been utilized as electrocatalysts for water splitting studies to tackle the energy related issues in our society. PANI and tungstic acid hybrid was annealed in a vacuum to produce a tungsten carbide/carbon composite by C. Liu *et al.*[135] The synthesized catalyst was utilized for electrocatalytic hydrogen evolution reaction (HER) studies. The composite showed an overpotential (OP) of 220 mV at 10 mA cm^{-2} and a Tafel slope value of 93 mV dec^{-1}. Iron-doped PANI was synthesized to evaluate the overall water-splitting efficiency and showed an OP of 235 mV for oxygen evolution reaction (OER) studies.[136] C. Ray *et al.* utilized PANI to synthesize nitrogen-doped cobalt–nickel nitride on carbon cloth for an overall water-splitting reaction. The OPs shown by this electrocatalyst at 10 mA cm^{-2} for HER and OER were 68 and 247 mV, respectively.[137]

Molybdenum carbide combined with nitrogen-doped carbon matrix was utilized for electrocatalytic HER studies. The study was carried out in both acidic and alkaline electrolytes, and the catalyst showed OPs of 81 and 89 mV in the alkaline and acidic mediums.[138] Nitrogen-doped carbon–iron phosphide composite was used as the catalyst for overall water splitting studies. It showed an OP of 193 mV for HER and 302 mV for OER studies. The potential required to reach a C_D of 10 mA cm^{-2} when a two electrode assembly, formed for overall water splitting, was found to be 1.63 V.[139] R. Djara *et al.* studied the effect of variation in the concentration of oxidants and doping agents utilized for the chemical oxidative synthesis of PANI towards HER analysis. It was found that when HCl was used as a doping agent and ammonium persulfate as the oxidant, the lowest OP of 690 mV was observed.[140] Thermal activation of PANI/GO and ammonium hexafluorophosphate was carried out to obtain N, P, and F-doped graphene, which was used for electrochemical water splitting studies. This composite showed an OP of 520 mV at a C_D of 10 mA cm^{-2}.[141]

A carbon nanostructured PANI–nickel composite was synthesized through a chemical oxidative polymerization technique and evaluated for HER and OER activity. OPs of 190 mV and 360 mV were shown by this catalyst for HER and OER, respectively.[142] Nickel–cobalt metal phosphide-coated PANI composite was utilized for HER study and showed an OP of 80.6 mV at a C_D of 10 mA cm^{-2}.[143] Carbon dots combined with PANI were explored for overall water splitting. The OER studies showed that an OP of 150 mV was required to reach a C_D of 30 mA cm^{-2}. In the case of HER, the OP required to reach a C_D of 20 mA cm^{-2} was found to be 65 mV (Fig. 8).[144]

PANI was combined with iridium for HER studies, which required an OP of 36 mV to reach a C_D of 10 mA cm^{-2}. PANI combined with ruthenium was utilized for OER study, which required an OP of 240 mV. An overall potential of 1.45 V was required by the catalyst when overall water splitting was carried out.[145] PANI combined with nickel–iron layered double hydroxide was utilized for OER studies, which utilized an OP of 220 mV, with a Tafel slope of 44 mV dec^{-1}.[146] Cobalt molybdenum sulfide/PANI composite required OPs of 98 and 250 mV at 10 mA cm^{-2} for HER and OER, respectively. The efficiency of this composite was due to the presence of a defect-rich structure and the conductive nature of PANI that directs the electron transfer.[147] Cobalt-incorporated PANI was analyzed for the OER study using glassy carbon and nickel foam substrates. When glassy carbon was used, an OP of 341 mV was required, whereas when nickel foam was used, the OP was reduced to 251 mV.[148] Cobalt-doped tungsten selenide/PANI composite required OPs of 308 and 360 mV for HER and OER analyses, respectively.[149] When cobalt-doped molybdenum selenide was combined with PANI, OPs of 196 and 385 mV were required for HER and OER, respectively.[150] The onset potential for OER was found to be 134 mV when zinc–cobalt/cellulose acetate/PANI composite was

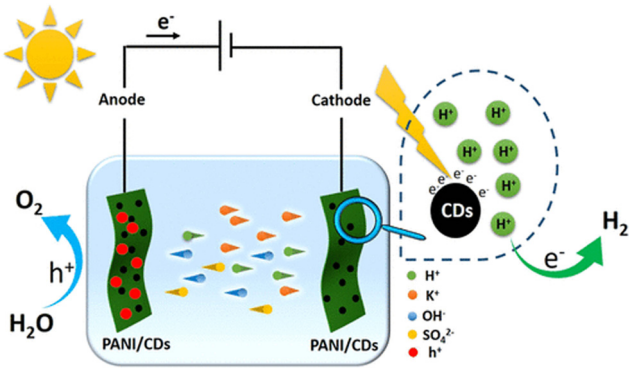

Fig. 8 Overall water splitting studies using PANI/carbon dot composite. Reproduced from ref. 144 with permission from ACS, copyright 2021.

used as an electrocatalyst.[151] When sulfonated PANI was combined with cobalt, an OP of 312 mV was required for OER analysis.[152] Copper molybdenum sulfide particles combined with rGO/PANI were utilized for OER, which required an OP of 395 mV.[153]

The metal oxides were combined with PANI in various studies to be used as the electrocatalysts for water splitting studies. PANI/manganese molybdenum oxide composite was utilized for overall water splitting studies. The OPs required for HER and OER studies were 155 mV and 410 mV, respectively, for the composite.[154] PANI/tungsten trioxide composite required an OP of 289 mV at 50 mA cm^{-2} for OER study.[155] PANI was combined with cobalt oxide to analyze its efficiency towards OER, and it required an OP of 258 mV to attain a C_D of 10 mA cm^{-2}.[156] Molybdenum/carbon/nickel electrocatalyst synthesized from PANI/molybdenum oxide was utilized for HER studies. The catalyst showed an onset potential of 44 mV at 1 mA cm^{-2}. The Tafel slope value was found to be 49 mV dec^{-1}, and the OP value was found to be 60 mV. The authors claim this is a potential earth-abundant catalyst for hydrogen generation.[157]

PANI and its composites have shown notable electrocatalytic activity in both the HER and OER. Pristine PANI exhibits a high HER OP (690 mV), indicating limited catalytic efficiency. However, upon hybridization with suitable materials, significant reductions in OP are observed. For instance, PANI/carbon dots (65 mV for HER, 150 mV for OER), PANI/nickel–cobalt phosphide (80.6 mV for HER), and PANI/tungstic acid (220 mV for HER) display marked improvements, illustrating the role of synergistic effects and enhanced active surface area. For OER, PANI/nickel (360 mV) and PANI/manganese molybdenum oxide (410 mV) show promising performance. The inclusion of multimetallic oxides, phosphides, and carbon-based nanostructures improves conductivity, boosts active site availability, and facilitates electron transfer, making PANI-based composites efficient bifunctional catalysts for overall water splitting.

Polyaniline composites for adsorption studies

The high surface area and excellent porous nature of PANI have made it an excellent adsorbent substance for removing toxic organic substances that cause pollution from water sources. The incorporation of substances like metal oxides into the PANI matrix has improved the adsorptive nature of PANI. Wood dust was used to synthesize ZnO through the green synthetic method, and it was incorporated into PANI for adsorptive removal studies of red-XGRL dye. 200 mg L^{-1} of the dye solution was used, and the optimum pH for the composite was 11. The composite showed a maximum adsorption capacity of 70.4 mg g^{-1} toward the dye solution. The study confirmed the fitness towards pseudo second order kinetics, Langmuir adsorption isotherm, and exothermic behavior of the adsorption process.[158] PANI/ZnO composite was synthesized using wheat straw and was used for the adsorptive removal of blue-XGRRL dye. The composite showed a maximum adsorption capacity of 55.8 mg g^{-1} towards a dye solution with a concentration of 100 mg L^{-1}. The adsorption process followed pseudo second order kinetics and Langmuir adsorption isotherm.[159]

In another study, PANI/ZnO adsorbent was chemically synthesized using formic acid. This composite was utilized to remove methylene orange dye from wastewater. Maximum removal efficiency of 97% was shown by the adsorbent within a period of 40 min.[160] Methyl orange dye removal was carried out by using PANI/ZnO composite, synthesized by A. Deb *et al.*[161] The maximum adsorption capacity was found to be 240.8 mg g^{-1}. When ultrasonication was carried out, the adsorption equilibrium was obtained within 15 min, which proves the efficiency of the ultrasonication method in the adsorption process. Using response surface methodology, the maximum removal efficiency of methyl orange dye was found to be 99%.

The synthesis of PANI/manganese oxide/niobium pentoxide composite was carried out using the chemical oxidative polymerization technique in an acidic medium. This was used as the adsorbent for the removal of methyl orange from an aqueous solution, which showed a maximum removal efficiency of 97.3%.[162] PANI was combined with iron oxide to remove basic blue dye from water samples. A maximum adsorption capacity of 78.1 mg g^{-1} was shown by the composite. The adsorption process followed pseudo second order kinetics. It was also found that the adsorption process is exothermic in nature.[163] Acid blue 40 dye was removed from water sources using PANI/iron oxide adsorbent. A higher maximum adsorption capacity of 216.9 mg g^{-1} was observed for this composite.[164] PANI/iron oxide was also used for the removal of chromium and nickel ions from the wastewater.[165]

Various organic pollutants like *p*-nitrophenol and resorcinol were removed from the wastewater by using PANI/nickel oxide composite. Freundlich and Temkin adsorption isotherms were best fitted for the process, and it followed pseudo second order kinetics. A maximum adsorption capacity of 19.53 mg g^{-1} for resorcinol and 29.78 mg g^{-1} for *p*-nitrophenol was observed.[166] PANI was combined with titanium dioxide to remove methyl orange dye. In this study, physical adsorption occurred between the dye molecules and the adsorbent.[167] In another study, polyacrylonitrile/PANI/TiO_2 fiber composite was synthesized through the electrospinning method. The Langmuir adsorption isotherm was the best fit for the adsorption process between congo red dye and the adsorbent. This membrane was also used to remove chromium ions from water sources.[168]

Nickel oxide and manganese oxide were incorporated into PANI to remove methyl orange dye through chemical oxidative polymerization of aniline using ammonium persulfate as the oxidant. Pure PANI has a removal efficiency of 53%, whereas the metal oxides-doped PANI showed an enhanced removal efficiency of 97%. The maximum adsorption capacity of metal oxides doped PANI was found to be 248.4 mg g^{-1}.[169] Iron, manganese, and zirconium oxides were combined with PANI for the removal studies of methyl red dye. A maximum adsorption capacity of 434.7 mg g^{-1} was seen for the adsorbent.[170] PANI/CuO/ZnO composite was synthesized to carry out the adsorptive removal of congo red dye. The negative values for the Gibbs free energy data suggest the spontaneity of the adsorption process.[171] Iron oxide, zirconium oxide, and manganese ferrite were incorporated into the PANI matrix to study

the adsorptive efficiency of a dye solution containing methyl orange and eosin yellow dyes.[172] Hollow PANI combined with manganese dioxide and iron oxide has been utilized for the adsorptive removal of malachite green and congo red dyes (Fig. 9).[173] From the studies, it is understood that PANI is an excellent candidate for various energy and environmental applications. Table 2 gives details of the adsorption studies reported using polymer composites.

Polypyrrole composites for energy and environmental applications

PPy was successfully synthesized by Donald Weiss and his team in 1963. In 1915, Angelo Angeli had already reported the synthesis of Pyrrole black, which was the early form of PPy.[174] The good conducting nature, electrochemical behavior, and excellent surface area of PPy have allowed scientists to use composites with PPy for energy applications.

Polypyrrole composites for supercapacitance studies

Introducing metal oxides into PPy has improved the efficiency of composites in applications for energy storage. The incorporation of molybdenum oxide into the PPy matrix was studied by M. Sun *et al.* The high C_{SP} and layered structure of this transition metal oxide, along with the fast charging–discharging capacity of PPy makes it an efficient candidate in charge storage applications.[175] Bismuth oxide was also utilized to combine with PPy composite to be used as an electrode for supercapacitance study. The electrolyte used in this study was lithium sulfate, and the C_S shown by this compound was found to be 360 F g^{-1}.[176] Gadolinium oxide was combined with PPy and polyindole to check the supercapacitance activity. It was found that the activity of the PPy composite was comparatively higher than that of the polyindole composite. The PPy composite showed a C_{SP} of 341.6 F g^{-1}, whereas the polyindole composite showed a lesser C_{SP} of 305.5 F g^{-1}. The GCD curves of this study confirm the pseudocapacitance nature of this composite.[177] Manganese oxide on carbon cloth was utilized as the cathode, and the PPy/Mxene composite was utilized as the anode in a study to form asymmetric supercapacitors. This

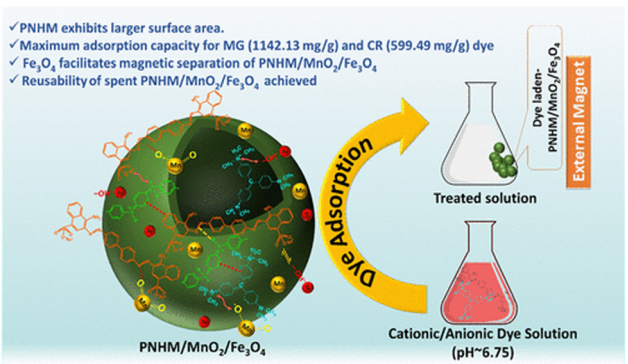

Fig. 9 Adsorptive studies using PANI/manganese dioxide/iron oxide on toxic dyes. Reproduced from ref. 173 with permission from ACS, copyright 2021.

Table 2 Reported works on the adsorption studies using polymers

Sl. no.	Composite	Dye	Maximum adsorptive capacitance (mg g^{-1})	Ref.
1	PANI/zinc oxide	RedXGRL	78.4	151
2	PANI/zincoxide	BlueXGRRL	55.8	152
3	PANI/zinc oxide	Methyl orange	240.8	154
4	PANI/iron oxide	Basic blue	78.1	156
5	PANI/iron oxide	Acid blue 40	216.9	157
6	PANI/nickel oxide	Resorcinol	19.5	159
7	PANI/nickel oxide/ manganese oxide	Methyl orange	248.4	162

fabricated energy storage device gave a C_{SP} of 75.3 F g^{-1} at a scan rate of 10 mV s^{-1}.[32] Iron oxide combined with PPy on carbon cloth showed a C_{SP} of 640 F g^{-1} at 1 mA cm^{-2}.[101] Iron oxide derived from the used ink cartridges is combined with PPy, which showed a C_{SP} of 319 F g^{-1} when a 4 M KOH was used as the electrolyte.[100]

Cobalt oxide, which is flower shaped, was combined with PPy and showed a C_{SP} of 6.81 F cm^{-2} at a C_D of 5 mA cm^{-2}. It also demonstrated a capacitance retention of 95% at 1000 cycles.[178] PPy, when combined with nickel oxide, has a C_{SP} of 595 F g^{-1} with a capacitance retention of 80.7% after 1000 cycles was observed.[179] PPy incorporated with vanadium pentoxide showed a C_{SP} of 172 F g^{-1}.[180] PPy was combined with honeycomb-like hematite to function as an electrode for studies related to storing energy. This PPy/iron oxide composite showed a C_{SP} of 1167.8 F g^{-1} at a C_D of 1 A g^{-1}. The retention of capacitance of this composite was studied for 3000 cycles, and it showed a capacitance retention of 97.1%.[181] Cobalt oxide, when combined with PPy, showed a C_{SP} of 155.5 mA h g^{-1}.[182] A highly porous cobalt oxide was combined with PPy for a supercapacitance study. The electrode made by this composite exhibited a C_{SP} of 1292.2 F g^{-1} at a C_D of 1 A g^{-1}.[183] In another study, porous iron oxide was incorporated into the PPy matrix, which produced an extensive conductive network for energy storage applications. This composite showed a C_{SP} of 215.12 mF cm^{-2} at 1.1 mA cm^{-2}.[184]

The carbon-based materials were also combined with PPy to act as electrodes for supercapacitance studies. Carbon nanotubes combined with PPy/manganese oxide showed a C_{SP} of 214 F g^{-1}. The carbon nanotube acted as flexible and conductive backing in this composite, whereas the role of metal oxide was to increase the surface area. The interface of PPy also plays a vital role in the energy storage activity of the composite.[185] Multiwalled carbon nanotube and manganese oxide were incorporated into the PPy matrix, which demonstrated a C_{SP} of 272.7 F g^{-1}.[186] PPy/manganese oxide/graphene/copper hydroxide composite was synthesized by H. N. Miankushki *et al.* In this study, the prepared composite showed a C_{SP} of 370 F g^{-1} in 6 M KOH solution.[187] PPy was combined with iron oxide and GO, which showed a C_{SP} of 163 F g^{-1} at 10 A g^{-1}. The electrolyte used in this study was lithium nitrate.[188] The study on the energy storage capacity of PPy/rGO doped manganese ferrite was carried out by S. Ishaq. It was found that the composite demonstrated a C_{SP} of 232 F g^{-1} at a scan rate of 5 mV s^{-1}.[189] One pot hydrothermal method was utilized to synthesize PPy/

rGO/cobalt oxide composite, which was used for supercapacitor applications. This study analyzed the influence of an anodic surfactant (sodium lauryl sulfate) on the synthesized composite. It was seen that with the addition of surfactant, the C_{SP} values increased from 1206 to 1663 F g^{-1}.[190] PPy/manganese oxide combined with carbon fiber paper was developed as a flexible supercapacitor with a C_{SP} of 69.3 F cm^{-3} (Fig. 10a–d).[191]

The ternary composites using PPy also showed good results in supercapacitance studies. Zinc oxide and tin oxide were combined with GO/PPy by V. Molahalli *et al.* The composite showed a C_{SP} of 392 F g^{-1} at a 75 mV s^{-1} scan rate.[192] The silver oxide was combined with PPy/Zn–Co MOF, which showed a C_{SP} of 420 F g^{-1} at a C_D of 1 A g^{-1}. This composite showed a cyclic stability of 84.5% capacitive retention after 10 000 cycles.[193] In another study, PPy was combined with rGO and iron oxide, which gave C_{SP} of 442 F g^{-1} at a C_D of 1 A g^{-1}.[194] Nitrogen–sulfur co-doped iron oxide was combined with PPy for supercapacitor applications. The C_{SP} demonstrated by this composite was 866 F g^{-1} at 1 A g^{-1}.[195] A co-electrodeposition method was carried out to synthesize PPy/nickel oxide/cobalt oxide in the form of nanosheets. The electrode using this composite demonstrated a C_{SP} of 1123 F g^{-1} at a C_D of 1 A g^{-1}.[196] PPy based composites showed efficiency in energy storage studies. Table 3 gives details of the supercapacitance studies reported using polymer composites.

PPy-based metal oxide composites have also exhibited excellent electrochemical behaviour, with certain combinations outperforming even their PANI counterparts. In particular, the PPy/rGO/cobalt oxide composite achieved an outstanding C_{SP} of 1663.0 F g^{-1}, followed by PPy/cobalt oxide (1292.2 F g^{-1}) and PPy/nickel oxide/cobalt oxide (1123.0 F g^{-1}), highlighting the efficiency of cobalt-rich systems in enhancing charge storage. The addition of nanostructured oxides, carbon nanotubes, and rGO to the PPy matrix facilitates improved electron transport, mechanical strength, and electroactive surface area. These findings underscore the versatility of PPy as a conductive polymer and its potential to be engineered with advanced nanostructures for sustainable and efficient supercapacitor applications.

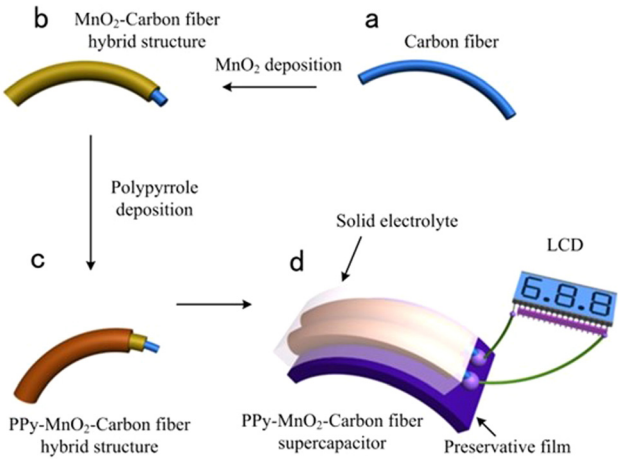

Fig. 10 Supercapacitance studies using a flexible PPy/manganese oxide combined with carbon fiber supercapacitor. Reproduced from ref. 191 with permission from Nature, copyright 2013.

Table 3 Reported works on the supercapacitance studies using polymers

Sl. no.	Composite	Specific capacitance (F g^{-1})	Ref.
1	PANI/iron oxide	286.0	93
2	PANI/copper oxide	376.0	102
3	PANI/manganese oxide	115.7	104
4	PANI/cobalt oxide	985.0	107
5	PANI/manganese oxide	665.0	110
6	PANI/zinc–cobalt oxide	1055.0	106
7	PANI/copper oxide-rGO	534.5	113
8	PANI/titanium oxide/tin oxide	540.0	114
9	PANI/manganese oxide/GO	829.0	115
10	PANI/ruthenium–cobalt oxide	1028.7	121
11	PANI/Ni–Co–Mn–MOF/rGO	1007.0	127
12	PPy/bismuth oxide	360.0	169
13	PPy/gadolinium oxide	341.6	170
14	PPy/cobalt oxide	1292.2	176
15	PPy/manganese oxide–carbon nanotubes	214.0	178
16	PPy/rGO/manganese ferrite	232.0	182
17	PPy/rGO/cobalt oxide	1663.0	183
18	PPy/nickel oxide/cobalt oxide	1123.0	189

Polypyrrole composites for water splitting studies

The water splitting studies were also carried out using various PPy based composites. Composites of PPy combined with metal oxides are reported for energy production studies. Samarium oxide was combined with PPy to be used as a bifunctional catalyst through the hydrothermal method for both HER and OER applications. The OPs required by the catalyst for HER and OER were observed as 206 and 272 mV at a C_D of 10 mA cm^{-2}.[197] Nickel/nickel ferrite combined with PPy was utilized for overall water splitting. The presence of PPy improves the rate of flow of ions and their interaction between the electrode and the electrolyte. The interaction between the conducting polymer and the nickel/nickel ferrite increases the reaction efficiency of the surface active sites. The OPs required for HER and OER by the catalyst were found to be 127 and 265 mV at a C_D of 10 mA cm^{-2}.[198] Cobalt oxide was combined with PPy for OER studies, and it showed an OP of 610 mV. The metal oxide enhances the electrocatalytic active surface area and electrochemical activity of the whole system.[199] When iridium oxide was combined with PPy, an OP of 291.3 mV was required to reach 10 mA cm^{-2}.[200] Nitrogen-doped carbon and cobalt oxide were combined and incorporated into PPy for electrochemical OER studies. This composite required an OP of 120 mV for OER analysis.[201] Nickel oxide was combined with PPy to be used as an electrocatalyst for OER analysis through the electrodeposition technique. It required an OP of 610 mV at a pH of 9.2.[202]

PPy was incorporated with walnut-shaped nickel hydroxide for OER studies. It showed an OP of 461 mV and a Tafel slope value of 89 mV dec^{-1}.[203] Flower shaped cobalt–nickel sulfide/PPy composite was synthesized for utilization in water splitting reactions. It was observed that the OPs required by the catalysts were 63 and 207 mV for HER and OER, respectively.[204] Iron–phosphorus nanorods were incorporated into PPy for HER

studies, which required an OP of 103.1 mV.[205] An electrodeposition technique was carried out for the synthesis of PPy, which was introduced with phosphotungstic anion on nickel foam. The OPs required by the catalyst were found to be 48 and 236 mV at a C_D of 10 mA cm^{-2} for HER and OER, respectively.[206] PPy was combined with iron, tungsten, and cobalt doped cobalt oxide for OER analysis, which showed an OP of 400 mV to reach 10 mA cm^{-2} C_D.[207] Cobalt phosphide containing PPy was utilized to synthesize N–O–P-doped hollow carbon composite through pyrolysis. This was utilized for HER analysis with an OP of 290 mV.[208] PPy/zinc tungstate was synthesized as a bifunctional electrocatalyst for water splitting with OPs of 76 and 84 mV towards Her and OER, respectively.[209]

In another study, PPy was combined with cobalt–nickel ferrite and rGO to obtain a catalyst for OER study. It required an OP of 371 mV for OER analysis.[210] Cobalt oxide incorporated PPy/carbon nanocomposite was utilized as an electrode material for water splitting, which required OPs of 340 and 490 mV for OER and HER, respectively.[211] PPy/ZIF-67 MOF was utilized for the synthesis of cobalt oxide/nitrogen-doped carbon nanotubes. The synthesized electrocatalyst required an OP of 200 mV for OER analysis.[212] PPy/cobalt hydroxide/rGO required an OP of 350 mV to attain a C_D of 10 mA cm^{-2} during OER analysis.[213] The combination of PPy with various metal oxides, heteroatoms, carbonaceous compounds, and MOFs enhances the properties of the polymer for water splitting studies. Table 4 gives details of the electrocatalytic water splitting studies reported using polymer composites.

PPy-based composites also exhibit promising HER and OER catalytic behavior. Notably, PPy/zinc tungstate demonstrates excellent bifunctional activity with very low OPs (76 mV for HER and 84 mV for OER), highlighting its efficiency. Other HER-active materials include PPy/nickel–nickel ferrite (127 mV) and PPy/samarium oxide (206 mV), while for OER, PPy/cobalt hydroxide/rGO (350 mV) and PPy/cobalt nickel ferrite/rGO (371 mV) display respectable values. However, some composites like PPy/cobalt oxide show a higher OER OP (610 mV), indicating room for improvement. The integration of rare-earth oxides, ferrites, and rGO into the PPy matrix enhances conductivity, electrochemical activity, and stability, confirming the viability of PPy-based composites for sustainable water electrolysis applications.

Table 4 Reported works on the electrocatalytic water splitting studies using polymers

Sl. No.	Composite	Overpotenital (mV) HER	OER	Ref.
1	PANI	690		133
2	PANI/tungstic acid	220		128
3	PANI/iron		235	129
4	Nitrogen doped-cobalt nickel nitride	68	247	130
5	PANI/nickel	190	360	135
6	PANI/nickel–cobalt phosphide	80.6		136
7	PANI/carbon dots	65	150	137
8	PANI/ruthenium		240	138
9	PANI/rGO/copper–molybdenum sulfide		395	146
10	PANI/manganese molybdenum oxide	155	410	147
11	PPy/samarium oxide	206	272	190
12	PPy/nickel–nickel ferrite	127	265	191
13	PPy/cobalt oxide		610	192
14	PPy/zinc tungstate	76	84	202
15	PPy/cobalt nickel ferrite/rGO		371	203
16	PPy/cobalt hydroxide/rGO		350	206
17	PPy/carbon–cobalt oxide	490	340	204

Other polymer composites for energy and environmental applications

Many other polymers like PEDOT, chitosan, and polythiophene were also reported for energy and environmental applications. The composites of these polymers were synthesized by incorporating various substances like metal oxides, carbonaceous compounds like graphene, and heteroatoms.

PEDOT composites

The supercapacitance studies using PEDOT based composites have caught the attention of researchers. A fiber-based supercapacitor was developed by combining PEDOT with vanadium pentoxide, showing a C_{SP} of 60 mF cm^{-2}.[214] Copper oxide nanowires were incorporated into the PEDOT matrix, which showed a remarkable C_{SP} of 907.5 mF cm^{-2} at a C_D of 3 mA cm^{-2}.[215] Cobalt ferrite was introduced into PEDOT to analyze the efficiency of charge storage capacity. It showed a C_S of 299.2 mA h g^{-1} at a C_D of 1 A g^{-1}. A cyclic stability of 91.7% capacitance retention was seen after 2000 cycles for this composite.[216] PEDOT, when combined with molybdenum oxide, shows a C_{SP} of 365 F g^{-1} at 1 A g^{-1}.[217] When iron oxide is incorporated into PEDOT, a C_{SP} of 338 mF cm^{-2} at a C_D of 1 mA cm^{-2} is obtained.[218] PEDOT was combined with tin oxide and evaluated for charge storage applications in 2 M sulphuric acid. The composite showed a C_{SP} of 126 F g^{-1}, which was evident from the GCD studies.[219] In 2014, cobalt oxide nanowires and manganese oxide were introduced into PEDOT to analyze its efficiency towards supercapacitor application.[220] In 2008, F. J. Liu introduced manganese oxide into PEDOT for energy storage studies. This composite showed a maximum C_{SP} of 372 F g^{-1}.[221] Manganese oxide is a common metal oxide used for various energy storage applications and is combined with PEDOT for synthesizing efficient composites for supercapacitance applications.[222–224]

When carbon nanotubes were introduced into PEDOT/MnO_2, an even higher C_{SP} of 427 F g^{-1} was obtained.[225] Iron oxide, when combined with graphene and PEDOT showed a C_{SP} of 153 F g^{-1} at 0.1 A g^{-1}. The cyclic stability was only seen up to 3500 cycles for this composite.[226] PEDOT/graphene/molybdenum oxide flexible supercapacitor was fabricated, and it showed a C_{SP} of 94 F g^{-1}. The role of PEDOT in this study was to behave as both a current collector and a binder.[102] When combined with titanium oxide and rGO, PEDOT showed a C_{SP} of 102.6 F g^{-1}. The binary rGO/titanium oxide in this study showed a C_{SP} of 98.8 F g^{-1}. The improvement in the C_{SP} of the final composite is due to the addition of a conducting polymer.[227] Nickel cobalt ferrite, when combined with rGO and PEDOT, gave a C_{SP} of 1286 F g^{-1}. The synergistic effect between the carbonaceous compound, conducting polymer,

and nickel cobalt ferrite is responsible for the better efficiency towards energy storage capacity.[228]

The HER studies using PEDOT composites were also reported. Pt/sulfonated graphene sheets/PEDOT were synthesized for HER analysis, and it was found that a lower OP of 40 mV was required to reach a C_D of 10 mA cm^{-2}. Even though the composite shows efficiency towards HER studies, the high cost of Pt makes it less feasible.[229] Pt/polyacrylic acid/PEDOT composite was utilized for HER analysis, which required an OP of 84 mV.[230] Cobalt–molybdenum selenide combined with PEDOT was utilized for overall water splitting. The OPs required for HER and OER were 20 and 153 mV, respectively.[231] Cobalt–nickel sulfide/PEDOT composite was also utilized as a bifunctional electrocatalyst, which required OPs of 90 and 270 mV for HER and OER, respectively.[232] The synergy between the various compounds incorporated into the polymer matrix and the PEDOT polymer has improved the electrochemical efficiency of the polymers.

Chitosan composites

The chitosan composites have been extensively used in anti-corrosion studies. There are also energy-related studies that have been reported using chitosan composites. The composites of chitosan with metal oxides are used for supercapacitance and water splitting studies. Chitosan/iron oxide combined with activated carbon was used as an electrode for supercapacitor application. This electrode showed a C_{SP} of 54.4 F g^{-1}.[233] Nitrogen-doped nickel oxide incorporated into porous carbon structure derived from nitrogen-doped chitosan was utilized for supercapacitance studies, which showed a C_{SP} of 614.6 F g^{-1}.[234] When combined with copper oxide and zinc oxide, chitosan showed a C_{SP} of 638.3 F g^{-1} and a capacitance retention of 86.98% at 5000 cycles.[235] Cobalt/nickel oxide combined with graphitic porous carbon composite was derived from chitosan and was utilized for energy storage studies. It showed a C_{SP} of 1266.7 F g^{-1} at a C_D of 1 A g^{-1}.[236] Copper oxide and copper metal were combined with chitosan to study the energy storage capacity, and it showed a C_{SP} of 2479 F g^{-1} at 0.5 A g^{-1}.[237] Nickel cobalt oxide sulfide used as an electrode for the supercapacitance study showed an energy density of 55.3 W h kg^{-1} at a power density of 400 W kg^{-1}.[238] Manganese cobalt oxide nanoneedle combined with carbon aerogel derived from chitosan showed an energy density of 84.3 W h kg^{-1} at a power density of 600 W kg^{-1}.[239]

The chitosan composites combined with metal oxides and heteroatoms were utilized for electrocatalytic water splitting studies. Nickel cobaltite combined with chitosan was utilized as the electrode for electrocatalytic water splitting. The OPs required for HER and OER were observed as 240 and 310 mV, respectively.[240] In another study, manganese cobalt oxide was combined with chitosan for the water splitting reaction. The overall water splitting reaction required a potential of 1.57 V to reach a C_D of 10 mA cm^{-2}. The OPs required for HER and OER were found to be 180 and 258 mV, respectively.[241] Chitosan/Prussian blue nanocomposite was coated on nickel foam to be used as an electrocatalyst for water-splitting studies. It was observed that OPs of 146 and 272 mV were required for HER and OER analysis, respectively, to reach a C_D of 10 mA cm^{-2}.[242] Chitosan combined with nickel oxide required an OP of 240 mV for OER analysis.[243] Nitrogen-doped chitosan matrix with tungsten oxide was utilized for overall water splitting, with OPs of 60 and 306 mV towards HER and OER, respectively.[244]

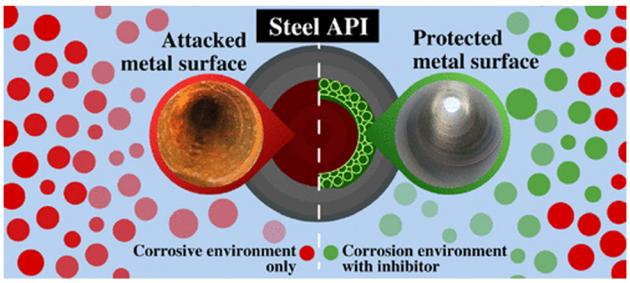

Fig. 11 Illustration of the inhibition action on metal surface. Reproduced from ref. 245 with permission from ACS, copyright 2024.

Chitosan is a polymer that is extensively used for corrosion inhibition studies. Many studies have reported using various chitosan composites for mitigating the corrosion effect. The inhibitors prevent the metal surface from undergoing corrosion (Fig. 11).[245] The chitosan was evaluated as an inhibitor on mild steel under acidic conditions, which showed an inhibition efficiency of 77%.[103] The combination of chitosan and metal oxides has been proven as an effective candidate in corrosion inhibition studies. Chitosan/TiO_2 composite was utilized as an inhibitor on mild steel under acidic conditions, which showed an inhibition efficiency of 97.1%.[246] Chitosan was combined with iron oxide to evaluate its efficiency in an acidic medium. The medium used was 15% HCl, and the composite showed an inhibition efficiency of 95.4%.[246] When copper oxide was combined with chitosan, the inhibition efficiency was 90.3% when studied under a 5% HCl medium on carbon steel.[63] Chitosan/GO/zinc oxide composite was evaluated for corrosion inhibition, and an inhibition efficiency of 85.6% was found in 1 M HCl solution. Thus, it is understood that the combination of polymers with suitable materials will enhance the efficiency towards energy and environmental applications.

Conclusions

This review discussed the importance of polymer based composites for energy and environmental applications. Polymer-based composites have shown significant promise in advancing energy and environmental technologies. Their customizable properties, including high surface area and conductivity, have led to notable improvements in energy storage within supercapacitors. In the realm of water splitting, these composites have enhanced catalytic efficiency, thereby supporting more effective hydrogen production. When applied to adsorption, polymer composites exhibit high selectivity and capacity for removing pollutants, making them highly effective for water treatment and environmental cleanup. Likewise, in corrosion inhibition, the incorporation of polymers into composite

materials offers a sustainable and efficient solution for protecting metal surfaces. These diverse applications highlight the flexibility and potential of polymer-based composites in tackling critical energy and environmental challenges.

The future of polymer-based composites in energy and environmental applications depends on advancing their performance through innovative material design and fabrication methods. Breakthroughs in nanotechnology, molecular engineering, and hybrid systems are expected to yield composites with greater efficiency and multifunctionality. Additionally, developing biodegradable and renewable polymers will be crucial for aligning these materials with sustainability objectives. Ensuring that these composites are scalable, cost-effective, and ready for real-world applications will be key to moving them from the lab to industry. As the demand for clean energy and environmental solutions continues to grow, polymer-based composites are set to play a pivotal role in shaping next-generation technologies.

Author contributions

Arun Varghese (Scopus ID-57205701115, ORCiD-0000-0002-6298-6739) conceptualization, data curation, methodology, writing – original draft. Kalathiparambil Rajendra Pai Sunajadevi (Scopus ID-55450509500, ORCiD-0000-0001-7826-1620) investigation, supervision, writing – reviewing and editing. Dephan Pinheiro (Scopus ID-57203248645, ORCiD-0000-0002-1921-248X) writing – reviewing and editing.

Data availability

The data will be made available on request.

Conflicts of interest

There are no conflicts to declare.

Acknowledgements

The authors are thankful to Christ University for providing the resources and facilities.

References

1 P. Wang, H. Wang, W.-Q. Chen and S. Pauliuk, *Fundam. Res.*, 2022, **2**, 392–395.
2 U. Riaz, S. M. Ashraf and J. Kashyap, *Polym. – Plast. Technol. Eng.*, 2015, **54**, 1850–1870.
3 N. K. Daniel, A. Varghese, K. R. Sunaja Devi, S. J. Chundattu and A. Sreekanth, *Colloids Surf., A*, 2024, **703**, 135177.
4 Z. Wang and B. Mi, *Environ. Sci. Technol.*, 2017, **51**, 8229–8244.
5 K. P. Chaitra, T. P. Vinod, A. Varghese and K. R. Sunajadevi, *Chem. Eng. J.*, 2024, **499**, 156049.
6 M. I. A. Abdel Maksoud, R. A. Fahim, A. E. Shalan, M. Abd Elkodous, S. O. Olojede, A. I. Osman, C. Farrell, A. H. Al-Muhtaseb, A. S. Awed, A. H. Ashour and D. W. Rooney, *Environ. Chem. Lett.*, 2021, **19**, 375–439.
7 A. Boretti, *Int. J. Hydrogen Energy*, 2022, **47**, 14371–14374.
8 T. H. Le, Y. Kim and H. Yoon, *Polymers*, 2017, **9**(4), 150.
9 G. Joseph, S. D. Kalathiparambil Rajendra Pai, A. Varghese, D. Pinheiro, M. K. Mohan and S. J. Chundattu, *J. Mol. Struct.*, 2024, **1308**, 138095.
10 A. Varghese and S. Devi K R, *Adv. Sustainable Syst.*, 2024, **2300575**, 1–11.
11 *Sustainable Development Goals: Their Impacts on Forests and People*, ed. P. Katila, C. J. Pierce Colfer, W. de Jong, G. Galloway, P. Pacheco and G. Winkel, Cambridge University Press, 2019.
12 J. D. Sachs, G. Schmidt-Traub, M. Mazzucato, D. Messner, N. Nakicenovic and J. Rockström, *Nat. Sustainable*, 2019, **2**, 805–814.
13 W. Schramade, *J. Appl. Corp. Financ.*, 2017, **29**, 87–99.
14 L. Wang, Y. Zhang, L. Chen, H. Xu and Y. Xiong, *Adv. Mater.*, 2018, **30**, 1–12.
15 A. Fleming, R. M. Wise, H. Hansen and L. Sams, *Mar. Policy*, 2017, **86**, 94–103.
16 R. B. Swain, A Critical Analysis of the Sustainable Development Goals, in *Handbook of Sustainability Science and Research*, ed. W. Leal Filho, World Sustainability Series, Springer, Cham, 2018, pp. 341–355.
17 S. Peter, N. Lyczko, D. Gopakumar, H. J. Maria, A. Nzihou and S. Thomas, *Waste Biomass Valorization*, 2021, **12**, 4777–4804.
18 L. S. Anthony, M. Vasudevan, V. Perumal, M. Ovinis, P. B. Raja and T. N. J. I. Edison, *J. Environ. Chem. Eng.*, 2021, **9**, 105832.
19 X. Zhao, L. Lv, B. Pan, W. Zhang, S. Zhang and Q. Zhang, *Chem. Eng. J.*, 2011, **170**, 381–394.
20 D. Lasrado, S. Ahankari and K. Kar, *J. Appl. Polym. Sci.*, 2020, 48959.
21 S. S. Siwal, Q. Zhang, N. Devi and V. K. Thakur, *Polymers*, 2020, **12**, 505.
22 T. A. Saleh, N. P. Shetti, M. M. Shanbhag, K. Raghava Reddy and T. M. Aminabhavi, *Mater. Sci. Energy Technol.*, 2020, **3**, 515–525.
23 S. Kulandaivalu, *Energies*, 2019, **12**, 2107.
24 A. G. Olabi, M. A. Abdelkareem, T. Wilberforce and E. T. Sayed, *Renewable Sustainable Energy Rev.*, 2021, **135**, 110026.
25 J. Theerthagiri, R. A. Senthil, P. Nithyadharseni, S. J. Lee, G. Durai, P. Kuppusami, J. Madhavan and M. Y. Choi, *Ceram. Int.*, 2020, **46**, 14317–14345.
26 Z. S. Iro, C. Subramani and S. S. Dash, *Int. J. Electrochem. Sci.*, 2016, **11**, 10628–10643.
27 J. Banerjee, K. Dutta, M. A. Kader and S. K. Nayak, *Polym. Adv. Technol.*, 2019, **30**, 1902–1921.
28 A. Dutta, S. Mitra, M. Basak and T. Banerjee, *Energy Storage*, 2022, **5**(1), e339.
29 R. Vinodh, R. S. Babu, S. Sambasivam, C. V. V. M. Gopi, S. Alzahmi, H.-J. Kim, A. L. F. de Barros and I. M. Obaidat, *Nanomaterials*, 2022, **12**, 1511.

30 A. Varghese, K. R. Sunaja Devi, S. Mathew, B. Saravanakumar and D. Pinheiro, *Mater. Today Proc.*, 2023, DOI: 10.1016/j.matpr.2023.12.003.
31 A. Varghese, S. Devi K R, F. Kausar and D. Pinheiro, *Mater. Today Chem.*, 2023, **29**, 101424.
32 X. Li, H. Xie, Y. Feng, Y. Qu, L. Zhai, H. Sun, X. Liu and C. Hou, *J. Mater. Sci.: Mater. Electron.*, 2023, **34**, 1878.
33 T. Jayaraman, A. P. Murthy, V. Elakkiya, S. Chandrasekaran, P. Nithyadharseni, Z. Khan, R. A. Senthil, R. Shanker, M. Raghavender, P. Kuppusami, M. Jagannathan and M. Ashokkumar, *J. Ind. Eng. Chem.*, 2018, **64**, 16–59.
34 Z. Yin and Q. Zheng, *Adv. Energy Mater.*, 2012, **2**, 179–218.
35 A. Varghese, K. Rajendra, P. Sunajadevi, D. Pinheiro, B. Saravanakumar and M. Selvaraj, *Int. J. Hydrogen Energy*, 2025, **123**, 238–246.
36 F. Kausar, A. Varghese, D. Pinheiro and S. Devi K R, *Int. J. Hydrogen Energy*, 2022, **47**, 22371–22402.
37 B. You and Y. Sun, *Acc. Chem. Res.*, 2018, **51**, 1571–1580.
38 X. Peng, C. Pi, X. Zhang, S. Li, K. Huo and P. K. Chu, *Sustainable Energy Fuels*, 2019, **3**, 366–381.
39 A. Varghese, S. Devi K R and D. Pinheiro, *Int. J. Hydrogen Energy*, 2023, **48**(76), 29552–29564.
40 X. Luo, X. Tan, P. Ji, L. Chen, J. Yu and S. Mu, *EnergyChem*, 2023, **5**, 100091.
41 S. Ji, Z. Yang, C. Zhang, Z. Liu, W. W. Tjiu, I. Y. Phang, Z. Zhang, J. Pan and T. Liu, *Electrochim. Acta*, 2013, **109**, 269–275.
42 S. Anantharaj, S. R. Ede, K. Karthick, S. Sam Sankar, K. Sangeetha, P. E. Karthik and S. Kundu, *Energy Environ. Sci.*, 2018, **11**, 744–771.
43 X. Chen, J. Yang, Y. Cao, L. Kong and J. Huang, *ChemElectroChem*, 2021, **8**, 4427–4440.
44 M. Nemiwal, T. C. Zhang and D. Kumar, *Int. J. Hydrogen Energy*, 2021, **46**, 21401–21418.
45 A. Varghese, S. Devi K R, D. Pinheiro and M. K. Mohan, *Surf. Interfaces*, 2023, **41**, 103221.
46 P. P. Nayak, A. Varghese, S. Devi K R and D. Pinheiro, *J. Appl. Polym. Sci.*, 2024, **141**, 1–12.
47 G. Ö. Kayan and A. Kayan, *J. Polym. Environ.*, 2021, **29**, 3477–3496.
48 A. Kayan, *Adv. Compos. Hybrid Mater.*, 2019, **2**, 34–45.
49 S. Jadoun, J. P. Fuentes, B. F. Urbano and J. Yáñez, *J. Environ. Chem. Eng.*, 2023, **11**, 109226.
50 M. Ahmadian and M. Jaymand, *Coord. Chem. Rev.*, 2023, **486**, 215152.
51 S. Samsami, M. Mohamadizaniani, M.-H. Sarrafzadeh, E. R. Rene and M. Firoozbahr, *Process Saf. Environ. Prot.*, 2020, **143**, 138–163.
52 S. Mathew, A. Varghese, S. Devi K. R. and D. Pinheiro, *Next Sustainable*, 2024, **4**, 100049.
53 A. Y. W. Sham and S. M. Notley, *J. Environ. Chem. Eng.*, 2018, **6**, 495–504.
54 A. Varghese, K. R. Sunaja Devi and D. Pinheiro, *Mater. Today Commun.*, 2023, **35**, 105739.
55 P. E. Ohale, K. Chukwudi, J. N. Ndive, M. E. Michael, M. N. Abonyi, M. M. Chukwu, C. C. Obi, C. E. Onu, C. A. Igwegbe and C. O. Azie, *Results Surf. Interfaces*, 2023, **13**, 100157.
56 J. P. Gaspard, *Interfacial Aspects of Phase Transformations*, Springer Netherlands, Dordrecht, 1982, pp. 103–118.
57 S. Singh, S. Perween and A. Ranjan, *J. Environ. Chem. Eng.*, 2021, **9**, 105149.
58 M. T. Rahman, T. Kameda, S. Kumagai and T. Yoshioka, *React. Kinet., Mech. Catal.*, 2017, **120**, 703–714.
59 Z. Wang, X. Wang and Y. Yang, *Adv. Mater.*, 2024, **36**(4), 2301721.
60 M. T. Baig and A. Kayan, *Int. J. Biol. Macromol.*, 2024, **280**, 135676.
61 A. Intisar, A. Ramzan, S. Hafeez, N. Hussain, M. Irfan, N. Shakeel, K. A. Gill, A. Iqbal, M. Janczarek and T. Jesionowski, *Chemosphere*, 2023, **336**, 139203.
62 H. Wang, D. Gao, Y. Meng, H. Wang, E. Wang and Y. Zhu, *Prog. Org. Coat.*, 2015, **82**, 74–80.
63 P. S. Umoren, D. Kavaz and S. A. Umoren, *Sustainability*, 2022, **14**, 7981.
64 A. K. Keerthana and P. M. Ashraf, *Appl. Nanosci.*, 2020, **10**, 1061–1071.
65 L. Guo, W. Dong and S. Zhang, *RSC Adv.*, 2014, **4**, 41956–41967.
66 S. John, A. Joseph, M. Kuruvilla and T. Sajini, *J. Bio-Tribo-Corrosion*, 2017, **3**, 3.
67 A. Varghese, K. R. Sunaja Devi, D. Pinheiro and J. Jomy, *J. Environ. Chem. Eng.*, 2024, 113824.
68 Q. Wang, R. Wang, Q. Zhang, C. Zhao, X. Zhou, H. Zheng, R. Zhang, Y. Sun and Z. Yan, *Molecules*, 2023, **28**, 2832.
69 P. Kesari, G. Udayabhanu, A. Roy and S. Pal, *Int. J. Biol. Macromol.*, 2023, **225**, 1323–1349.
70 W. v Baeckmann, *Handbook of Cathodic Corrosion Protection*, Elsevier, 1997, pp. 1–26.
71 S. Sivakumar, P. K. Selvaraj and S. Selvaraj, *Asian J. Chem.*, 2018, **30**, 2043–2048.
72 H. R. Bakhsheshi-Rad, E. Hamzah, W. S. Ying, M. Razzaghi, S. Sharif, A. F. Ismail and F. Berto, *Materials*, 2021, **14**, 1930.
73 P. D. Desai, C. B. Pawar, M. S. Avhad and A. P. More, *Vietnam J. Chem.*, 2023, **61**, 15–42.
74 X. Lu, W. Zhang, C. Wang, T. Wen and Y. Wei, *Prog. Polym. Sci.*, 2011, **36**, 671–712.
75 C. K. Chiang, S. C. Gau, C. R. Fincher, Y. W. Park and A. G. Macdiarmid, *Phys. Rev. Lett.*, 1977, **39**, 1098–1101.
76 S. Mallakpour, M. Dinari and E. Azadi, *Int. J. Polym. Anal. Charact.*, 2015, **20**, 82–97.
77 Y. Li, Y. Yu, L. Wu and J. Zhi, *Appl. Surf. Sci.*, 2013, **273**, 135–143.
78 K. M. Ismayil, A. Varghese and R. Antony, *J. Elastomers Plast.*, 2020, **52**, 103–116.
79 C. Ramesh, M. Hariprasad, V. Ragunathan and N. Jayakumar, *Eur. J. Appl. Eng. Sci. Res.*, 2012, **1**, 201–206.
80 X. Zang, R. Jiang, H.-Y. Zhu, Q. Wang, Y.-Q. Fu, D.-X. Zhao, J.-B. Li and H. Liu, *Sep. Purif. Technol.*, 2024, **330**, 125521.
81 D. Tekin, D. Birhan and H. Kiziltas, *Mater. Chem. Phys.*, 2020, 123067.

82 M. Deifallah, P. F. McMillan and F. Corà, *J. Phys. Chem. C*, 2008, **112**, 5447–5453.
83 X. Zhou, F. Peng, H. Wang, H. Yu and Y. Fang, *Chem. Commun.*, 2011, **47**, 10323–10325.
84 X. Liu and L. Cai, *Appl. Surf. Sci.*, 2018, **445**, 242–254.
85 R. Nekooie, T. Shamspur and A. Mostafavi, *J. Photochem. Photobiol., A*, 2021, **407**, 113038.
86 S. Rajendran, R. Pachaiappan, T. K. A. Hoang, S. Karthikeyan, L. Gnanasekaran, S. Vadivel, M. Soto-Moscoso and M. A. Gracia-Pinilla, *J. Hazard. Mater.*, 2021, **416**, 125989.
87 S. Vignesh, S. Suganthi, J. Kalyana Sundar, V. Raj and P. R. Indra Devi, *Appl. Surf. Sci.*, 2019, **479**, 914–929.
88 H. Ahmed, A. Hashim and H. M. Abduljalil, *Egypt. J. Chem.*, 2019, **62**, 1167–1176.
89 M. Soleimani, M. Ghorbani and S. Salahi, *Int. J. Nanosci. Nanotechnol.*, 2016, **12**, 191–197.
90 G. Sharma, D. Pathania, M. Naushad and N. C. Kothiyal, *Chem. Eng. J.*, 2014, **251**, 413–421.
91 I. Shown, A. Ganguly, L. C. Chen and K. H. Chen, *Energy Sci. Eng.*, 2015, **3**, 2–26.
92 W. Raza, F. Ali, N. Raza, Y. Luo, K. Kim and J. Yang, *Nano Energy*, 2018, **52**, 441–473.
93 V. Kumaravel, S. C. Pillai and P. Forouzandeh, *Catalysts*, 2020, **10**, 969.
94 G. Zhao, X. Huang, Z. Tang, Q. Huang, F. Niu and X. Wang, *Polym. Chem.*, 2018, **9**, 3562–3582.
95 D. Duranoğlu, I. G. Buyruklardan Kaya, U. Beker and B. F. Ş enkal, *Chem. Eng. J.*, 2012, **181–182**, 103–112.
96 L. Li, Z. Wang, P. Ma, H. Bai, W. Dong and M. Chen, *J. Polym. Res.*, 2015, **22**, 1–10.
97 R. C. Patil and S. Radhakrishnan, *Prog. Org. Coat.*, 2006, **57**, 332–336.
98 H. Albaris and G. Karuppasamy, *J. Mater. Sci.: Mater. Electron.*, 2019, **30**, 9989–9998.
99 Q. W. Zengyuan Pang, Q. Nie, P. Lv, J. Yu and F. Huang, *IOPscience*, 2017, **2**, 0–31.
100 P. M. Jambhale, V. N. Narwade, M. Shariq, K. A. Bogle and M. D. Shirsat, *J. Electron. Mater.*, 2024, **53**, 3117–3127.
101 C. Wu, Z. Pei, M. Lv, D. Huang, Y. Wang and S. Yuan, *Molecules*, 2023, **28**, 434.
102 S. L. Marasso, P. Rivolo, R. Giardi, D. Mombello, A. Gigot, M. Serrapede, S. Benetto, A. Enrico, M. Cocuzza, E. Tresso and C. F. Pirri, *Mater. Res. Express*, 2016, **3**, 065001.
103 M. Srivastava, S. K. Srivastava, Nikhil, G. Ji and R. Prakash, *Int. J. Biol. Macromol.*, 2019, **140**, 177–187.
104 S. C. Rasmussen, *An Int. J. Hist. Chem. Subst.*, 2017, **1**, 99–109.
105 G. A. Snook, P. Kao and A. S. Best, *J. Power Sources*, 2011, **196**, 1–12.
106 M. Ayad and S. Zaghlol, *Chem. Eng. J.*, 2012, **204–205**, 79–86.
107 U. Gazal, I. Khan, M. A. Usmani and A. H. Bhat, *Polymer-based Nanocomposites for Energy and Environmental Applications*, Elsevier, 2018, pp. 315–332.
108 R. Sun, Y. Pei, H. Ren, Y. Jin, J. Hu, Q. Wang, X. Wang and M. Yan, *J. Appl. Polym. Sci.*, 2023, **141**(12), e55111.
109 P. Supchocksoonthorn, S. Witchakul, W. Pholauyphon, T. Jorn-am, P. Janpauk, N. Sirisit, X. Liang, S. Song, T. Sangtawesin and P. Paoprasert, *J. Power Sources*, 2023, **587**, 233724.
110 D. J. Ahirrao and N. Jha, *AIP Conf. Proc.*, 2017, **1832**, 050168.
111 D. A. L. Almeida, C. O. P. Silva, D. A. Graves, R. M. Sanches, R. C. Firmino, A. F. Sardinha, N. G. Ferreira, M. Gonçalves, A. C. C. Migliano and E. S. Gonçalves, *Electrochim. Acta*, 2023, **472**, 143369.
112 S. P. Ashokkumar, H. Vijeth, L. Yesappa, M. Niranjana, M. Vandana and H. Devendrappa, *Inorg. Chem. Commun.*, 2020, **115**, 107865.
113 B. Zhou, Z. Li, D. Qin, Q. Zhang, M. Yu and C. Yang, *J. Alloys Compd.*, 2023, **956**, 170327.
114 I. I. Misnon, K. Manickavasakam, N. Nordin and R. Jose, *Int. J. Appl. Ceram. Technol.*, 2023, **20**, 2030–2042.
115 Y. Wang, Y. Wang, C. Wang and Y. Wang, *J. Compos. Sci.*, 2021, **5**, 129.
116 T. Prasankumar, B. R. Wiston, C. R. Gautam, R. Ilangovan and S. P. Jose, *J. Alloys Compd.*, 2018, **757**, 466–475.
117 M. M. Mezgebe, K. Xu, G. Wei, S. Guang and H. Xu, *J. Alloys Compd.*, 2019, **794**, 634–644.
118 C. P. Sandhya, R. Baig E, S. Pillai, C. Molji, A. Aravind and S. J. Devaki, *Electrochim. Acta*, 2019, **324**, 134876.
119 D. Qin, B. Zhou, Z. Li and C. Yang, *J. Mol. Struct.*, 2024, **1309**, 138140.
120 L. He, J. Liu, L. Yang, Y. Song, M. Wang, D. Peng, Z. Zhang and S. Fang, *Electrochim. Acta*, 2018, **275**, 133–144.
121 R. Bolagam, R. Boddula and P. Srinivasan, *ChemistrySelect*, 2017, **2**, 65–73.
122 K. Y. Yasoda, M. S. Kumar and S. K. Batabyal, *Ionics*, 2020, **26**, 2493–2500.
123 G. Singh, Y. Kumar and S. Husain, *Energy Storage*, 2024, **6**, e525.
124 Y. Ma, Y. Fu, N. Wei, J. Zhu, H. Niu, C. Qin and X. Jiang, *J. Appl. Polym. Sci.*, 2023, **140**, e54672.
125 X. Li, H. Xie, Y. Feng, Y. Qu, L. Zhai, H. Sun, X. Liu and C. Hou, *J. Appl. Polym. Sci.*, 2023, **140**, e54580.
126 S. Vargheese, G. Dhakal, R. S. Kumar, R. T. R. Kumar, J.-J. Shim and Y. Haldorai, *J. Energy Storage*, 2023, **71**, 108145.
127 R. Kalpana and P. Subbramaniyan, *Int. Res. J. Multidiscip. Technovation*, 2024, 40–50.
128 T. Kavinkumar, T. R. Naveenkumar and B. Neppolian, *J. Alloys Compd.*, 2024, **982**, 173741.
129 A. S. Almalki, *J. Mater. Sci.: Mater. Electron.*, 2024, **35**, 581.
130 S. Sahoo, G. Dhakal, W. K. Kim, Y. R. Lee and J.-J. Shim, *J. Energy Storage*, 2023, **73**, 109061.
131 A. R. Athira, T. Merin, K. Anupama, K. A. Ann Mary and T. S. Xavier, *Diamond Relat. Mater.*, 2022, **130**, 109475.
132 M. Naveed, T. Munawar, M. Shahid, F. Mukhtar, A. Maqbool, M. Riaz, S. Manzoor, M. Naeem and F. Iqbal, *Ceram. Int.*, 2021, **47**, 18497–18509.
133 Y. Sui, Y. Ma, Y. Gao, J. Song, Y. Ye, H. Niu, W. Ma, P. Zhang and C. Qin, *New J. Chem.*, 2021, **45**, 10654–10663.
134 M. A. Marwat, S. Ishfaq, K. M. Adam, B. Tahir, M. H. Shaikh, M. F. Khan, M. R. Abdul Karim, Z. U. Din,

S. Abdullah and E. Ghazanfar, *RSC Adv.*, 2024, **14**, 2102–2115.
135 C. Liu, J. Zhou, Y. Xiao, L. Yang, D. Yang and D. Zhou, *Int. J. Hydrogen Energy*, 2017, **42**, 29781–29790.
136 Y. Dong, J. Feng and G. Li, *Macromol. Chem. Phys.*, 2017, **18**(22), 1700359.
137 C. Ray, S. C. Lee, B. Jin, A. Kundu, J. H. Park and S. Chan Jun, *J. Mater. Chem. A*, 2018, **6**, 4466–4476.
138 J.-T. Ren, L. Chen, C.-C. Weng, G.-G. Yuan and Z.-Y. Yuan, *ACS Appl. Mater. Interfaces*, 2018, **10**, 33276–33286.
139 J. Tong, T. Li, L. Bo, W. Li, Y. Li and Y. Zhang, *ChemElectroChem*, 2019, **6**, 3437–3444.
140 R. Djara, Y. Holade, A. Merzouki, N. Masquelez, D. Cot, B. Rebiere, E. Petit, P. Huguet, C. Canaff, S. Morisset, T. W. Napporn, D. Cornu and S. Tingry, *J. Electrochem. Soc.*, 2020, **167**, 066503.
141 J. Zhang and L. Dai, *Angew. Chem., Int. Ed.*, 2016, **55**, 13296–13300.
142 R. Djara, Y. Holade, A. Merzouki, M.-A. Lacour, N. Masquelez, V. Flaud, D. Cot, B. Rebiere, A. van der Lee, J. Cambedouzou, P. Huguet, S. Tingry and D. Cornu, *Front. Chem.*, 2020, **8**, 385.
143 J. Zhang, Y. Li, Z. Wang, Y. Wang, F. Wang and M. Chen, *Nanotechnology*, 2020, **31**, 445401.
144 X. Gu, Z. Chen, Y. Li, J. Wu, X. Wang, H. Huang, Y. Liu, B. Dong, M. Shao and Z. Kang, *ACS Appl. Mater. Interfaces*, 2021, **13**, 24814–24823.
145 R. Djara, M.-A. Lacour, A. Merzouki, J. Cambedouzou, D. Cornu, S. Tingry and Y. Holade, *Polymers*, 2021, **13**, 190.
146 J. Zhang, H. Zhang and Y. Huang, *Appl. Catal., B*, 2021, **297**, 120453.
147 S. Mathew, J.-H. Sim, R. Rajmohan, O. L. Li and Y.-R. Cho, *Electrochim. Acta*, 2022, **403**, 139586.
148 S. Sriram, S. Mathi, B. Vishnu, B. Karthikeyan and J. Jayabharathi, *ChemistrySelect*, 2022, **7**(8), e202104516.
149 S. Cogal, G. Celik Cogal, M. Mičušík, M. Kotlár and M. Omastová, *Int. J. Hydrogen Energy*, 2024, **49**, 689–700.
150 S. Cogal, G. Celik Cogal, M. Mičušík, A. Michalcova, M. Šlouf and M. Omastová, *J. Electroanal. Chem.*, 2023, **946**, 117728.
151 M. W. Fazal, F. Zafar, M. Asad, F. Mohammad, H. Al Sulami, H. Khalid, A. A. Abdelwahab, M. U. Ur Rehman, N. Akhtar, W. A. El-Said, S. Hussain and M. A. Shenashen, *ACS Appl. Energy Mater.*, 2023, **6**, 2739–2746.
152 M. Vijayarangan, S. Mathi, A. Gayathri, J. Jayabarathi and V. Thanikachalam, *ChemistrySelect*, 2022, **7**(43), e202203206.
153 A. Singh, A. Singh, G. Kociok-Köhn, R. Bhimireddi, A. Singh, A. K. Singh, A. Kumar and M. Muddassir, *Appl. Organomet. Chem.*, 2022, **36**(6), e6683.
154 M. S. Tamboli, S. A. Patil, A. M. Tamboli, S. S. Patil, N. T. N. Truong, K. Lee, C. S. Praveen, N. K. Shrestha, C. Park and B. B. Kale, *Dalton Trans.*, 2022, **51**, 6027–6035.
155 A. M. Alenad, T. A. M. Taha, M. Abdullah, A. G. Abid, S. Manzoor, R. Y. Khosa, H. M. T. Farid, S. Trukhanov, M. I. Sayyed, D. Tishkevich and A. Trukhanov, *J. Electroanal. Chem.*, 2023, **941**, 117550.
156 S. S. Dakave, G. A. Bhinge, N. N. Kengar, A. D. Teli and C. M. Kanamadi, *Mater. Today Proc.*, 2023, DOI: 10.1016/j.matpr.2022.12.246.
157 J. Zhang, X. Meng, J. Zhao and Z. Zhu, *ChemCatChem*, 2014, **6**, 2059–2064.
158 T. Aliyam, R. Munir, G. Albasher, M. Zahid, T. Samreen, M. Ghamkhar, M. Yaseen, F. Younas and S. Noreen, *Polym. Bull.*, 2024, **81**, 8251–8284.
159 T. Aliyam, R. Munir, G. Albasher, M. Yaseen, M. Zahid, M. Shakeel and S. Noreen, *Colloid Polym. Sci.*, 2024, **302**, 409–431.
160 S. M. Alardhi, A. H. Abdalsalam, A. A. Ati, M. H. Abdulkareem, A. A. Ramadhan, M. M. Taki and Z. Y. Abbas, *Polym. Bull.*, 2024, **81**, 1131–1157.
161 A. Deb, M. Kanmani, A. Debnath, K. L. Bhowmik and B. Saha, *Ultrason. Sonochem.*, 2019, **54**, 290–301.
162 K. M. Obaid, A. S. Abbas and Y. F. Al-Khafaji, *Indones. J. Chem.*, 2023, **23**, 1270.
163 A. Muhammad, A.-H. A. Shah, S. Bilal and G. Rahman, *Materials*, 2019, **12**, 1764.
164 A. Muhammad, A. ul H. A. Shah and S. Bilal, *Materials*, 2019, **12**, 2854.
165 A. Muhammad, A. ul H. A. Shah and S. Bilal, *Appl. Sci.*, 2020, **10**, 2882.
166 B. Goswami and D. Mahanta, *Colloids Surf., A*, 2019, **582**, 123843.
167 J. N. Ramteke, N. V. Nerkar and S. B. Kondawar, *Springer Proceedings in Physics*, 2020, *242*, pp. 87–94.
168 B. Xu, X. Wang, Y. Huang, J. Liu, D. Wang, S. Feng, X. Huang and H. Wang, *Chem. Eng. J.*, 2020, **399**, 125749.
169 L. I. A. Ali, H. K. Ismail, H. F. Alesary and H. Y. Aboul-Enein, *Int. J. Environ. Sci. Technol.*, 2021, **18**, 2031–2050.
170 B. Saha, A. Debnath and B. Saha, *J. Indian Chem. Soc.*, 2022, **99**, 100635.
171 T. B. Gelaw, B. K. Sarojini and A. K. Kodoth, *J. Polym. Environ.*, 2022, **30**, 4086–4101.
172 A. Deb, A. Debnath, K. Bhowmik, S. Rudra Paul and B. Saha, *Int. J. Environ. Anal. Chem.*, 2023, **103**, 5938–5956.
173 S. Dutta, S. K. Srivastava, B. Gupta and A. K. Gupta, *ACS Appl. Mater. Interfaces*, 2021, **13**, 54324–54338.
174 C. Rasmussen Seth, *Bull. Hist. Chem.*, 2015, **40**, 45–55.
175 M. Sun, Y. Zhang, Z. Liang, R. Zhang, K. Zhang, Y. Lin, D. Wang and T. Xie, *New J. Chem.*, 2024, **48**, 6723–6732.
176 E. Karaca, *J. Energy Storage*, 2023, **71**, 108210.
177 Y. Senjaliya, N. Oad, S. Chakroborty, B. Tripathi, P. Chandra, P. K. Tripathi, A. Solanki, I. A. Darwish, S. Rawat, A. Barik, R. Kapadia and N. Asthana, *J. Mol. Struct.*, 2024, **1307**, 137919.
178 X. Wang, L. Jia, Q. Liu, J. Liu, X. Guo, X. Jing and J. Wang, *Colloids Surf., A*, 2016, **506**, 646–653.
179 W. Ji, J. Ji, X. Cui, J. Chen, D. Liu, H. Deng and Q. Fu, *Chem. Commun.*, 2015, **51**, 7669–7672.
180 X. Sun, Q. Li and Y. Mao, *Electrochim. Acta*, 2015, **174**, 563–573.
181 P.-Y. Tang, L.-J. Han, A. Genç, Y.-M. He, X. Zhang, L. Zhang, J. R. Galán-Mascarós, J. R. Morante and J. Arbiol, *Nano Energy*, 2016, **22**, 189–201.

182 C. Yang, H. Chen and C. Guan, *Nanomaterials*, 2019, **9**, 586.
183 Z. Zhang, X. Su, Y. Zhu, Z. Fang, X. Luo and Z. Chen, *Nanotechnology*, 2020, **31**, 255403.
184 Y. Xue, N. Gao, H. Ma, Y. Wang and C. Liu, *Mater. Today Commun.*, 2024, **40**, 109445.
185 P. Li, Y. Yang, E. Shi, Q. Shen, Y. Shang, S. Wu, J. Wei, K. Wang, H. Zhu, Q. Yuan, A. Cao and D. Wu, *ACS Appl. Mater. Interfaces*, 2014, **6**, 5228–5234.
186 A. H. P. de Oliveira, M. L. F. Nascimento and H. P. de Oliveira, *Mater. Res.*, 2016, **19**, 1080–1087.
187 H. N. Miankushki, A. Sedghi and S. Baghshahi, *J. Solid State Electrochem.*, 2018, **22**, 3317–3329.
188 C. R. Mariappan, V. Gajraj, S. Gade, A. Kumar, S. Dsoke, S. Indris, H. Ehrenberg, G. V. Prakash and R. Jose, *J. Electroanal. Chem.*, 2019, **845**, 72–83.
189 S. Ishaq, M. Moussa, F. Kanwal, M. Ehsan, M. Saleem, T. N. Van and D. Losic, *Sci. Rep.*, 2019, **9**, 5974.
190 A. R. Athira and T. S. Xavier, *J. Mater. Sci.: Mater. Electron.*, 2024, **35**, 509.
191 J. Tao, N. Liu, W. Ma, L. Ding, L. Li, J. Su and Y. Gao, *Sci. Rep.*, 2013, **3**, 2286.
192 V. Molahalli, V. S. Bhat, A. Shetty, D. Hundekal, A. Toghan and G. Hegde, *J. Energy Storage*, 2023, **69**, 107953.
193 Q. Wang, C. Han, G. Tang, L. Liu, T. Li and Y. Han, *J. Alloys Compd.*, 2023, **931**, 167510.
194 J. Vigneshwaran, S. Abraham, B. Muniyandi, T. Prasankumar, J. T. Li and S. Jose, *Surf. Interfaces*, 2021, **27**, 101572.
195 M. Zhu, Q. Chen, J. Tang, W. Wei and S. Li, *Appl. Surf. Sci.*, 2019, **480**, 582–592.
196 Z.-M. Shen, X.-J. Luo, Y.-Y. Zhu and Y.-S. Liu, *J. Energy Storage*, 2022, **51**, 104475.
197 A. M. Tawfeek, K. Jabbour, A. G. Abid, M. U. Nisa, S. Manzoor, B. Shabbir, M. Y. ur Rehman, T. Munawar, M. Sillanpää and M. N. Ashiq, *J. Sol-Gel Sci. Technol.*, 2024, DOI: 10.1007/s10971-023-06288-3.
198 L. Jia, G. Du, D. Han, Y. Wang, W. Zhao, Q. Su, S. Ding and B. Xu, *Chem. Eng. J.*, 2023, **454**, 140278.
199 D. V. Morales, C. N. Astudillo, V. Anastasoaie, B. Dautreppe, B. F. Urbano, B. L. Rivas, C. Gondran, D. Aldakov, B. Chovelon, D. André, J.-L. Putaux, C. Lancelon-Pin, S. Sirach, E.-M. Ungureanu, C. Costentin, M.-N. Collomb and J. Fortage, *Sustainable Energy Fuels*, 2021, **5**, 4710–4723.
200 J. Zhang, S. Liu, H. Wang, Q. Xia and X. Huang, *Int. J. Hydrogen Energy*, 2020, **45**, 33491–33499.
201 S. Farid, S. Ren, D. Tian, W. Qiu, J. Zhao, L. Zhao, Q. Mao and C. Hao, *Int. J. Hydrogen Energy*, 2020, **45**, 31926–31941.
202 D. V. Morales, C. N. Astudillo, Y. Lattach, B. F. Urbano, E. Pereira, B. L. Rivas, J. Arnaud, J.-L. Putaux, S. Sirach, S. Cobo, J.-C. Moutet, M.-N. Collomb and J. Fortage, *Catal. Sci. Technol.*, 2018, **8**, 4030–4043.
203 Q. Li, H. He, Z. Zheng, L. Zhang, J. Chen, S. Li, B. Zhang, J. Zhang, S. Luo and A. Xie, *Ionics*, 2022, **28**, 4341–4351.
204 Y. Song, P. Hong, T. Li, G. Ma, Q. Deng, Y. Zhou and Y. Zhang, *J. Colloid Interface Sci.*, 2022, **618**, 1–10.
205 H. Pei, L. Zhang, G. Zhi, D. Kong, Y. Wang, S. Huang, J. Zang, T. Xu, H. Wang and X. Li, *Chem. Eng. J.*, 2022, **433**, 133643.
206 L. Wu, J. Cen, A. Ali, J. Li and P. Kang Shen, *J. Electroanal. Chem.*, 2022, **904**, 115877.
207 Q. Hu, Y. Liu, L. Ma, X. Zhang and H. Huang, *J. Appl. Electrochem.*, 2018, **48**, 1189–1195.
208 S. Huang, Y. Meng, Y. Cao, S. He, X. Li, S. Tong and M. Wu, *Appl. Catal., B*, 2019, **248**, 239–248.
209 K. Brijesh, K. Bindu, D. Shanbhag and H. S. Nagaraja, *Int. J. Hydrogen Energy*, 2019, **44**, 757–767.
210 X. Jia, Y. Zhang, D. Guo, L. Zhang, L. Wang and L. Zhou, *Ionics*, 2020, **26**, 1885–1894.
211 S. S. Jayaseelan, N. Bhuvanendran, Q. Xu and H. Su, *Int. J. Hydrogen Energy*, 2020, **45**, 4587–4595.
212 S. Farid, W. Qiu, J. Zhao, X. Song, Q. Mao, S. Ren and C. Hao, *J. Electroanal. Chem.*, 2020, **858**, 113768.
213 H. Mao, X. Guo, Y. Fu, Z. Cao, D. Sun, B. Wang, Y. Zhang, Q. Fan and X.-M. Song, *Appl. Surf. Sci.*, 2019, **485**, 554–563.
214 Q. Xu, C. Lu, S. Sun and K. Zhang, *J. Phys. Chem. Solids*, 2019, **129**, 234–241.
215 A. Abas, H. Sheng, Y. Ma, X. Zhang, Y. Wei, Q. Su, W. Lan and E. Xie, *J. Mater. Sci.: Mater. Electron.*, 2019, **30**, 10953–10960.
216 K. Song, R. Yang, X. Chen, X. Wang, G. Chen and N. Zhao, *Appl. Surf. Sci.*, 2021, **542**, 148670.
217 S. Muduli, T. K. Pani, K. K. Garlapati and S. K. Martha, *J. Energy Storage*, 2024, **95**, 112396.
218 Y. Wang, T. Zhang, X. Zheng, X. Tian and S. Yuan, *ACS Appl. Mater. Interfaces*, 2023, **15**, 59413–59421.
219 M. Lee and J. Bae, *Bull. Korean Chem. Soc.*, 2015, **36**, 2101–2106.
220 X. Xia, D. Chao, Z. Fan, C. Guan, X. Cao, H. Zhang and H. J. Fan, *Nano Lett.*, 2014, **14**, 1651–1658.
221 F.-J. Liu, *J. Power Sources*, 2008, **182**, 383–388.
222 X. Shen, T. Wang, X. Wei and S. Li, *ACS Appl. Energy Mater.*, 2022, **5**, 2596–2605.
223 P. S. Shewale and K.-S. Yun, *J. Alloys Compd.*, 2022, **911**, 164939.
224 X. Shen, X. Wei, T. Wang, S. Li and H. Li, *Mater. Chem. Front.*, 2022, **6**, 2894–2904.
225 Y. Hou, Y. Cheng, T. Hobson and J. Liu, *Nano Lett.*, 2010, **10**, 2727–2733.
226 E. Pardieu, S. Pronkin, M. Dolci, T. Dintzer, B. P. Pichon, D. Begin, C. Pham-Huu, P. Schaaf, S. Begin-Colin and F. Boulmedais, *J. Mater. Chem. A*, 2015, **3**, 22877–22885.
227 R. Maharsi, A. F. Arif, T. Ogi, H. Widiyandari and F. Iskandar, *RSC Adv.*, 2019, **9**, 27896–27903.
228 K. Hareesh, S. R. Rondiya, N. Y. Dzade, S. D. Dhole, J. Williams and S. Sergey, *J. Sci.: Adv. Mater. Devices*, 2021, **6**, 291–301.
229 A. Abdolmaleki, Z. Mohamadi, A. A. Ensafi, N. Z. Atashbar and B. Rezaei, *Int. J. Hydrogen Energy*, 2018, **43**, 8323–8332.
230 A. J. Hackett, J. Malmström and J. Travas-Sejdic, *ACS Appl. Energy Mater.*, 2019, **2**, 1436–1444.
231 S. Cogal, S. Ramani, V. R. Bhethanabotla and J. N. Kuhn, *ChemCatChem*, 2021, **13**, 2017–2024.
232 H. Liu, D. Zhao, M. Dai, X. Zhu, F. Qu, A. Umar and X. Wu, *Chem. Eng. J.*, 2022, **428**, 131183.

233 A. Witecka, P. Pietrzyk-Thel, M. Krajewski, K. Sobczak, A. Wolska and A. Jain, *J. Alloys Compd.*, 2024, **985**, 174040.
234 K. Chen, J. Liu, H. Bian, J. Wei, W. Wang and Z. Shao, *Nanotechnology*, 2020, **31**, 335713.
235 M. Gouda, M. M. Khalaf, M. F. Abou Taleb and H. M. Abd El-Lateef, *J. Appl. Polym. Sci.*, 2024, 55293.
236 Y. Liu, C. Xiang, H. Chu, S. Qiu, J. McLeod, Z. She, F. Xu, L. Sun and Y. Zou, *J. Mater. Sci. Technol.*, 2020, **37**, 135–142.
237 Y. Xi, Z. Xiao, H. Lv, H. Sun, S. Zhai and Q. An, *J. Colloid Interface Sci.*, 2023, **630**, 525–534.
238 P. Hao, J. Tian, Y. Sang, C.-C. Tuan, G. Cui, X. Shi, C. P. Wong, B. Tang and H. Liu, *Nanoscale*, 2016, **8**, 16292–16301.
239 P. Hao, Z. Zhao, L. Li, C.-C. Tuan, H. Li, Y. Sang, H. Jiang, C. P. Wong and H. Liu, *Nanoscale*, 2015, **7**, 14401–14412.
240 S. S. Medany, A. Nafady, R. A. Soomro and M. A. Hefnawy, *Sci. Rep.*, 2024, **14**, 2453.
241 L. Xia, J. Wang, L. Bo, W. Shi, Y. Zhang, Y. Shen, X. Ji, X. Guan, Y. Wang and J. Tong, *Chem. Eng. J.*, 2023, **467**, 143464.
242 T. Dhanasekaran, A. Bovas and T. P. Radhakrishnan, *ACS Appl. Mater. Interfaces*, 2023, **15**, 6687–6696.
243 U. Divya Madhuri and T. P. Radhakrishnan, *ChemElectroChem*, 2019, **6**, 1984–1989.
244 J. Chen, H. Yang, X. Sang, Z. Su, D. Li and Q. Wang, *Solid State Sci.*, 2018, **83**, 23–30.
245 V. Díaz-Jiménez, G. Gómez-Sánchez, N. V. Likhanova, P. Arellanes-Lozada, O. Olivares-Xometl, I. V. Lijanova and J. Arriola-Morales, *ACS Omega*, 2024, **9**, 27798–27831.
246 P. Kesari, G. Udayabhanu, A. Roy and S. Pal, *Int. J. Biol. Macromol.*, 2023, **225**, 1323–1349.